

Low-lying $E1$, $M1$, and $E2$ strength distributions in $^{124,126,128,129,130,131,132,134,136}\text{Xe}$: Systematic photon scattering experiments in the mass region of a nuclear shape or phase transition

H. von Garrel,¹ P. von Brentano,² C. Fransen,² G. Friessner,² N. Hollmann,² J. Jolie,² F. Käppeler,³ L. Käubler,⁴ U. Kneissl,¹ C. Kohstall,¹ L. Kostov,^{4,*} A. Linnemann,² D. Mücher,² N. Pietralla,^{2,†} H. H. Pitz,¹ G. Rusev,⁴ M. Scheck,^{1,‡} K. D. Schilling,⁴ C. Scholl,² R. Schwengner,⁴ F. Stedile,¹ S. Walter,^{1,§} V. Werner,^{2,||} and K. Wisshak³

¹Institut für Strahlenphysik, Universität Stuttgart, D-70569 Stuttgart, Germany

²Institut für Kernphysik, Universität zu Köln, D-50937 Köln, Germany

³Institut für Kernphysik, Forschungszentrum Karlsruhe, D-76021 Karlsruhe, Germany

⁴Institut für Kern- und Hadronenphysik, Forschungszentrum Rossendorf, D-01314 Dresden, Germany

(Received 15 February 2006; published 31 May 2006)

Systematic nuclear resonance fluorescence (NRF) experiments on all nine stable (seven even-even and two odd-mass) Xe isotopes have been performed at the bremsstrahlung facility of the 4.3-MV Stuttgart Dynamitron accelerator. For the first time thin-walled, high-pressure gas targets (about 70 bar) with highly enriched target material were used in NRF experiments. Precise excitation energies, transition strengths, spins, and decay branching ratios were obtained for numerous states, most of them previously unknown. The systematics of the observed $E1$ two-phonon excitations ($2^+ \otimes 3^-$) and $M1$ excitations to 1^+ mixed-symmetry states in the even-even isotopes are discussed with respect to the new critical point symmetry E(5). The fragmentation of these fundamental dipole excitation modes in the odd-mass isotopes $^{129,131}\text{Xe}$ is shown and discussed. In the even-even nuclei several low-lying $E2$ excitations were observed.

DOI: 10.1103/PhysRevC.73.054315

PACS number(s): 27.60.+j

I. MOTIVATION AND INTRODUCTION

Nuclear shape or phase transitions are a current topic in nuclear structure physics. The properties of spherical, axially deformed, and γ -soft even-even nuclei can be described well in the framework of algebraic models in the dynamical symmetry limits of U(5), SU(3), and O(6) as is well known [1]. Moreover, Iachello introduced three new so-called critical point symmetries [2–4], which, for the first time, also allow descriptions of nuclei in the mass region of nuclear phase or shape transitions. The symmetries E(5), X(5), and Y(5) apply for nuclei at the critical points of phase transitions from spherical vibrators to deformed γ -soft nuclei, to axially symmetric deformed rotors, and from axially symmetric to rigidly triaxial rotors, respectively. Nuclei at critical points should exhibit, in comparison to their neighboring isotopes, dramatic changes in their structure and hence of the experimental observables, such as level schemes and orderings, γ -transition probabilities, and decay branchings. The first experimental evidence of these symmetries has been seen in $N = 90$ isotones [X(5)] [5–8], in ^{134}Ba [E(5)] [9], and possibly in $^{166,168}\text{Er}$ [Y(5)] [4].

Whereas the X(5) first-order phase/shape transition is clearly seen in the sudden onset of the deformation splitting of the higher lying $E1$ giant dipole resonance (GDR) in the chains of Sm and Nd isotopes [10,11] and is indicated in the abrupt concentration of the $M1$ scissors mode strength in ^{150}Nd [12–15], there is so far no evidence in dipole strength distributions for the predicted second-order E(5) phase transition. Our recent study of the even-even Ba isotopes $^{138,136,134}\text{Ba}$ [16–19] suffered in this respect from the fact that the other existing stable, very rare isotopes $^{132,130}\text{Ba}$ were not available in sufficient quantities (several grams) necessary for present-day photon scattering experiments.

Therefore, the aim of the present work was to study the influence of the E(5) shape or phase transition on low-lying $E1$ or $M1$ strength distributions in even-even Xe nuclei. Owing to the $N = 82$ shell closure there exist in the Xe isotopic chain seven stable even-even and two stable odd-mass isotopes, covering the extremely broad mass number range $A = 136 - 124$. Whereas ^{136}Xe ($N = 82$) is of a spherical shape, the lightest isotopes $^{126,124}\text{Xe}$ are considered as γ -soft nuclei [20,21].

One of the key quantities for the evidence of these symmetries is the ratio R of the excitation energies of the first 4^+ and 2^+ states in even-even nuclei. In Fig. 1 these ratios are plotted for nuclei near the $N = 82$ shell closure together with the values expected for U(5), E(5), O(6), and SU(3) nuclei. The data for the Xe isotopes are emphasized by full circles. Obviously, the Xe isotopic chain, with seven stable even-even isotopes, crosses the U(5), E(5) values and reaches the O(6) limit. Therefore, this chain provides a unique case to investigate systematically the changes of spectroscopic observables expected for shape or phase transitions near the critical points.

*Permanent address: Institute for Nuclear Research and Nuclear Energy, BAS, 1784 Sofia, Bulgaria.

†Present address: Department of Physics and Astronomy, State University of New York, Stony Brook, New York 11794-3800, USA.

‡Present address: Departments of Chemistry and Physics & Astronomy, University of Kentucky, Lexington, Kentucky 40506-0055, USA.

§Present address: Institut für Kernphysik, Forschungszentrum Karlsruhe, D-76021 Karlsruhe, Germany.

||Present address: WSNL, Yale University, 272 Whitney Avenue, New Haven, Connecticut 06520-8124, USA.

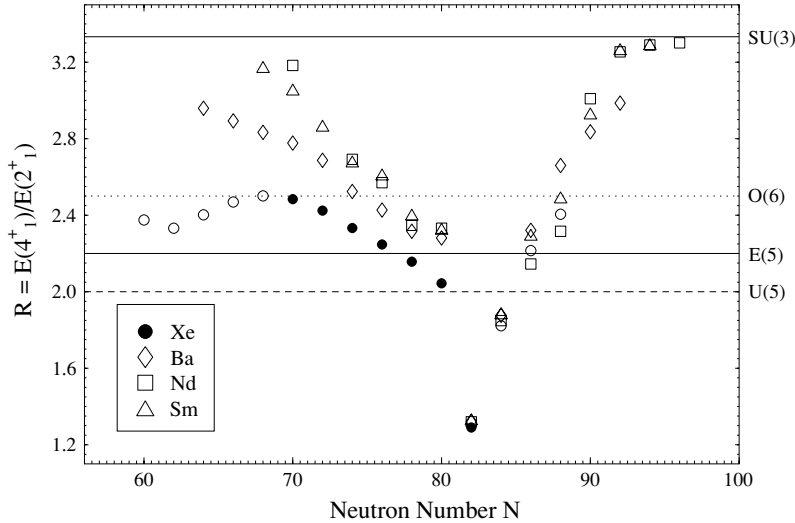


FIG. 1. Ratio R of the excitation energies $E(4_1^+)$ and $E(2_1^+)$ of the first excited 4^+ and 2^+ states in the even-even Xe, Ba, Nd, and Sm isotopes as a function of the neutron number N . The data points of the investigated stable Xe isotopes are emphasized by full symbols.

The paper is organized as follows. The basic formalism describing nuclear resonance fluorescence experiments is briefly summarized in Sec. II. The experimental setup at the Stuttgart Dynamitron accelerator and the high-pressure gas targets are described in Sec. III. The results are presented in Sec. IV. The discussion in Sec. V concentrates on four issues: the $E1$ two-phonon excitations, the $M1$ excitations to 1^+ mixed-symmetry states in the even-even isotopes, $E2$ excitations observed in the even-even isotopes, and the fragmentation of the dipole strength in the odd-mass isotopes.

II. THE NUCLEAR RESONANCE FLUORESCENCE METHOD

Nuclear resonance fluorescence (NRF), photon scattering off bound states, has proven to be the most sensitive technique to study low-lying dipole excitations in heavy nuclei, both of electric and magnetic character ([15] and references therein). Precise excitation energies E_x , ground-state transition widths Γ_0 , and decay branching ratios can be extracted from the spectra of the scattered photons measured in NRF experiments. These quantities can be converted into reduced transition probabilities $B(E1) \uparrow$ and $B(M1) \uparrow$ or lifetimes τ . For the favorable cases of even-even nuclei, additionally model-independent information on the spins and parities of the photo-excited levels can be deduced from angular distribution and linear polarization measurements (see Refs. [15,22]).

In bremsstrahlung-induced NRF experiments, owing to the continuous energy distribution of the photon beam, one automatically integrates over the narrow resonances. The corresponding total scattering intensity $I_{S,f}$, integrated over the full solid angle, is given by

$$I_{S,f} = g \left(\pi \frac{\hbar c}{E_x} \right)^2 \frac{\Gamma_0 \Gamma_f}{\Gamma}. \quad (1)$$

Here, Γ_0 , Γ_f , and Γ denote the decay widths of the excited state with spin J to the ground state with spin J_0 , that to the final level with spin J_f , and the total level width, respectively. For $\Gamma_0 = \Gamma_f$ one obtains the integrated cross section $I_{S,0}$ for

the decay back to the ground state:

$$I_{S,0} = g \left(\pi \frac{\hbar c}{E_x} \right)^2 \frac{\Gamma_0^2}{\Gamma}. \quad (2)$$

The statistical weight g , often called the spin factor, is given by $g = (2J + 1)/(2J_0 + 1)$. It is equal to 3 in the case of dipole excitations in even-even nuclei. The product $g \Gamma_0/E_x^3$ is directly proportional to the reduced excitation probabilities $B(\lambda L, E_x) \uparrow = B[\lambda L; J_0 \rightarrow J(E_x)]$, ($\lambda = E$ or M). For practice the following numerical relations are useful for electric or magnetic dipole excitations, respectively:

$$B(E1) \uparrow = 0.955 \frac{g \Gamma_0}{E_x^3} 10^{-3} e^2 \text{ fm}^2, \quad (3)$$

$$B(M1) \uparrow = 0.0864 \frac{g \Gamma_0}{E_x^3} \mu_N^2. \quad (4)$$

Here the excitation energies E_x should be taken in MeV and the ground-state transition widths Γ_0 in meV.

Unfortunately, for odd-mass nuclei the spins J and parities π of the photo-excited levels in most cases cannot be determined unambiguously in present-day NRF experiments because of the nearly isotropic angular distributions. Therefore, the spin factor g in general is not known. However, the quantity $g \Gamma_0^{\text{red}}$ with

$$\Gamma_0^{\text{red}} = \frac{\Gamma_0}{E_x^3}, \quad (5)$$

which is proportional to the corresponding reduced transition probabilities $B(\lambda 1) \uparrow$ [See Eqs. (3) and (4)] can be measured directly. Therefore, the reduced transition probabilities can be deduced even without knowledge of the spins J of the photo-excited states.

The decay branching ratios of the photo-excited states $R_{\text{exp},i}$ to lower lying excited levels labeled by i and to the ground state are defined as the ratio of the corresponding reduced transition probabilities (assuming pure dipole transitions)

$$R_{\text{exp},i} = \frac{B(\pi L; J \rightarrow J_i)}{B(\pi L; J \rightarrow J_0)} = \frac{\Gamma_i}{\Gamma_0} \cdot \frac{E_{\gamma 0}^3}{E_{\gamma i}^3}. \quad (6)$$

The branching ratios contain valuable additional information on the structure of the photo-excited states.

The formalism describing NRF experiments can be found in more detail in previous reviews [15,22].

III. EXPERIMENTAL DETAILS

A. Experiments at the Stuttgart Dynamitron

The NRF experiments on all stable Xe isotopes were carried out at the well-established bremsstrahlung facility installed at the 4.3-MV Dynamitron of Stuttgart University [15]. All measurements were performed at a bremsstrahlung end-point energy of 4.1 MeV. The DC electron currents used in the experiments had to be limited to about 250 μA , owing to the thermal capacity of the radiator target of about 1 kW. For all experiments, isotopically highly enriched targets were available. Times of data collection were between 3 and 6 days per isotope. In Table I target specifications, beam parameters, and measuring times of the present NRF experiments on ^{124}Xe , ^{126}Xe , ^{128}Xe , ^{129}Xe , ^{130}Xe , ^{131}Xe , ^{132}Xe , ^{134}Xe , and ^{136}Xe are summarized.

The scattered photons were detected by three well-shielded, high-resolution Ge γ -ray spectrometers installed at angles of about 90° , 127° , and 150° with respect to the incoming bremsstrahlung beam. Each of the detectors had an efficiency of about 100% relative to a standard $7.6\text{ cm} \times 7.6\text{ cm}$ NaI(Tl) detector. The energy resolutions were typically about 2 keV at a photon energy of 1.3 MeV and about 3 keV at 3 MeV. The detector at 127° was additionally surrounded by a BGO anti-Compton shield to improve its response function. Special high-pressure gas targets (see Sec. III B) were used for the first time in photon scattering experiments. The targets were attached to aluminum sheets. The isotope ^{27}Al , with some very well known excitations, serves generally in bremsstrahlung-induced NRF experiments as photon flux monitor [23].

B. The high-pressure gas targets

Gaseous isotopes, in particular those of the extremely long Xe isotopic chain, are of special interest for systematic nuclear structure studies. However, usually such gaseous isotopes were beyond the reach of present-day photon scattering experiments, since masses of at least some hundreds of milligrams of highly enriched target material are necessary for measurements of realistic running times of some days. To gain access to these isotopes one needs a small, high-pressure

gas target, preferably made from a low- Z container material. These requirements are met by a special target cell developed at the Forschungszentrum Karlsruhe for (n, γ) investigations of astrophysical relevance [24].

The Karlsruhe high-pressure Xe target consists of an electron-welded titanium sphere with a titanium valve. The diameter of the sphere, which has a wall thickness of only 0.2 mm, is 10.4 mm, and the empty weight is about 3 g. The sphere is filled with Xe up to a pressure of 70 bar. The maximum test pressure is about 140 bar. The filling is done by freezing. At room temperature xenon is an overcritical liquid; its critical temperature is 289.7 K. Above the critical temperature gases cannot be fluidized just by increasing the pressure. Therefore, there is no separation between liquid and gas and all the included target material is homogeneously distributed, a situation that is very advantageous for photon scattering experiments.

The target is especially well suited for photon scattering experiments, for several reasons. First, it enables one to bring in a small volume enough target material into the photon beam. Furthermore, its diameter is smaller than the photon beam cross section, so that all target material is hit by the beam. The nozzle ensures that the valve is outside of the beam. The container material titanium, besides its high mechanical stability, offers the advantage of a low atomic number Z , leading to a low nonresonant photon scattering background. Furthermore, in the most abundant Ti isotope, ^{48}Ti (74%), there exist only a few excitations in the energy range below 4 MeV, which in addition are well known from previous NRF experiments at Stuttgart [25].

Test measurements included runs with empty target cells and with natural Xe gas fillings. The specification of the targets with highly enriched Xe isotopes used in the present NRF experiments are summarized in Table I.

IV. RESULTS

A. Results for the even-even isotopes $^{124-136}\text{Xe}$

Precise excitation energies, transition strengths, spins, and decay branching ratios were obtained for numerous states, most of them unknown so far. Unfortunately, no parity assignments via Compton polarimetry [26] were possible in reasonable measuring times because of the low target quantities of less than 1 g.

Figure 2 gives an overview on the systematics of very clean (γ, γ') spectra observed for all investigated stable

TABLE I. Target specifications, beam parameters, and measuring times.

Isotope	^{124}Xe	^{126}Xe	^{128}Xe	^{129}Xe	^{130}Xe	^{131}Xe	^{132}Xe	^{134}Xe	^{136}Xe
Target mass (mg)	503	588 ^a	696	790	311	760	594	604	555
Enrichment (%)	≥ 99.9	≥ 99.9	99.6(1)	≥ 99.9	99.7(1)	≥ 99.5	≥ 99.9	≥ 99.9	94.4(1) ^b
^{27}Al mass (mg)	178	178	178	178	178	178	178	178	178
End-point energy (MeV)	4.1	4.1	4.1	4.1	4.1	4.1	4.1	4.1	4.1
Electron current (μA)	220	200	200	210	220	190	220	220	210
Measuring time (days)	4.1	4.5	3.7	6.0	5.0	3.1	4.3	3.9	5.1

^aAverage value (leakage loss of 22 mg during the measurement).

^bImpurity: 5.6% ^{134}Xe .

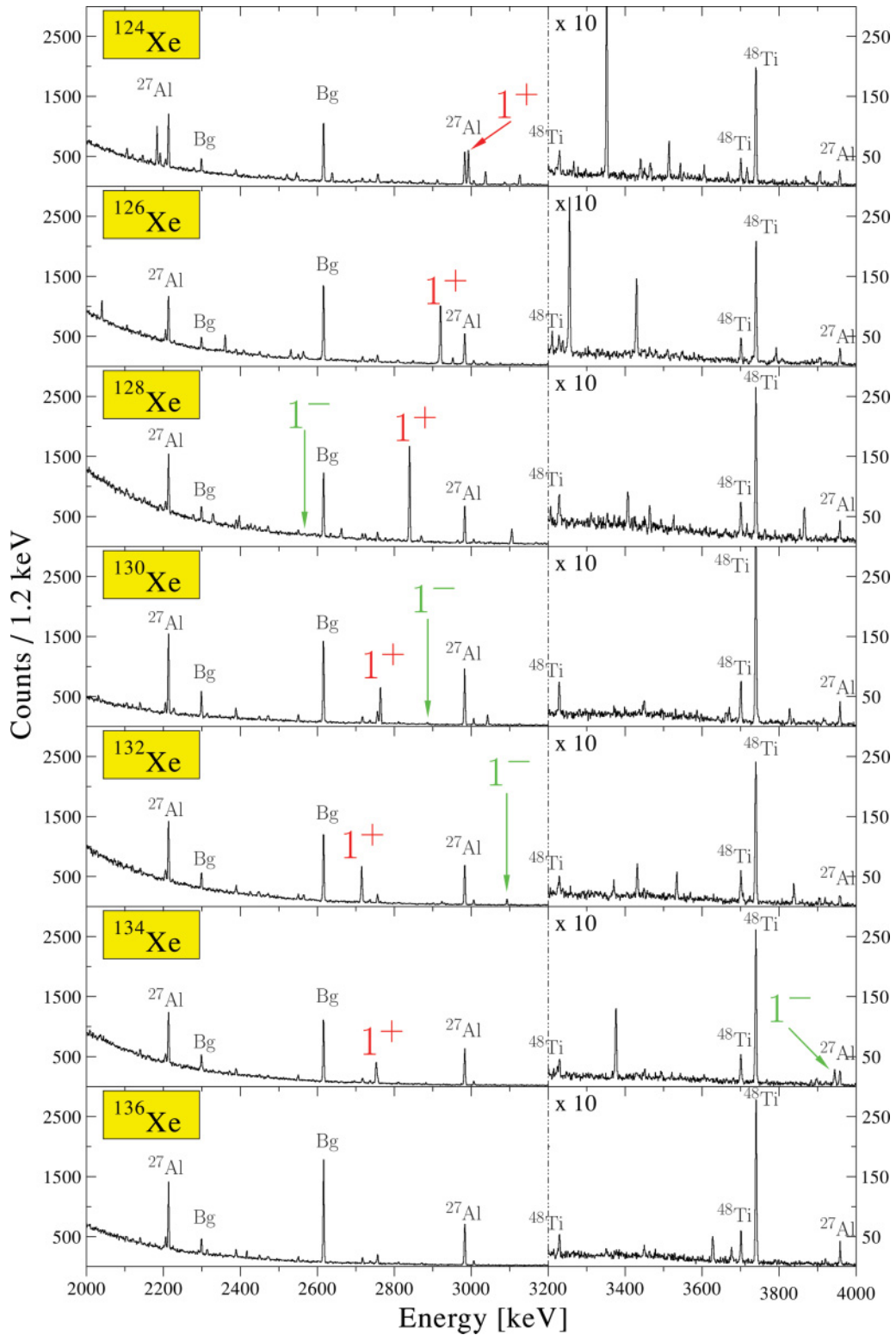


FIG. 2. (Color online) Systematics of (γ, γ') spectra observed for all stable even-even $^{124-136}\text{Xe}$ isotopes investigated in Stuttgart NRF experiments using a bremsstrahlung end-point energy of 4.1 MeV. Shown is the energy region where the $E1$ two-phonon excitations and 1^+ mixed-symmetry states are expected. Peaks attributed to these excitations are marked by 1^- and 1^+ . Peaks labeled by ^{27}Al , ^{48}Ti , or Bg belong to transitions in the aluminum photon flux calibration standard or in the titanium target container material or are background lines from the environmental radioactivity, respectively. In the energy range 3200–4000 keV the ordinate scale is enlarged by a factor of 10.

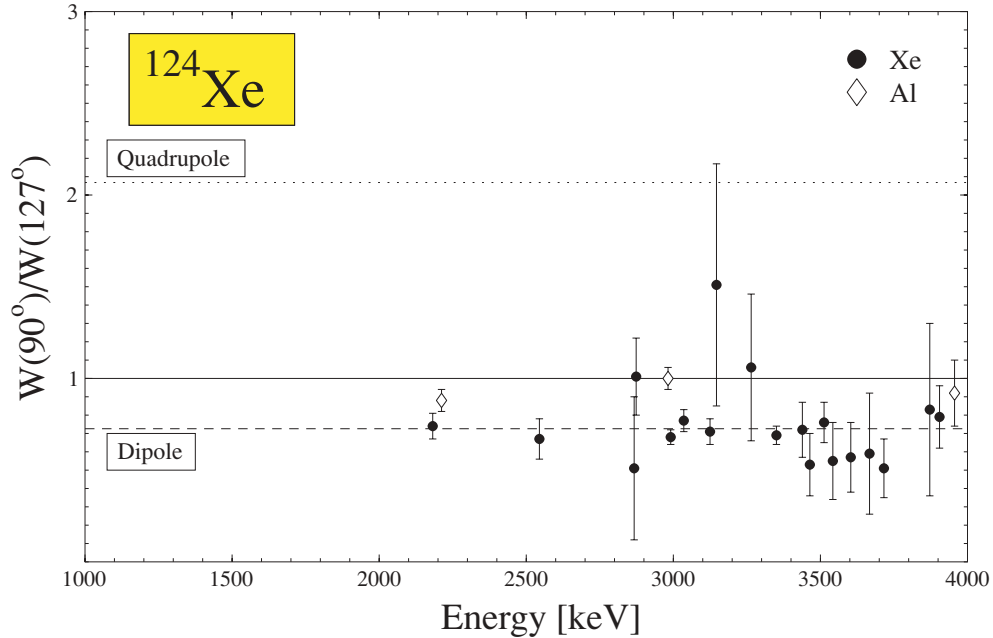


FIG. 3. (Color online) Results of the angular distribution measurements in the reaction $^{124}\text{Xe}(\gamma, \gamma')$. Plotted are the intensity ratios $W(90^\circ)/W(127^\circ)$ for the observed ground-state transitions. The dotted and dashed lines show the expected values for dipole and quadrupole transitions (spin sequences $0-1-0$ and $0-2-0$, respectively). The open diamonds show the ratios for the nearly isotropic transitions in ^{27}Al , normalized to unity for the 2982-keV transition in ^{27}Al .

even-even Xe isotopes $^{124-136}\text{Xe}$ as measured in Stuttgart NRF experiments using a bremsstrahlung beam with an end-point energy of 4.1 MeV. Marked peaks correspond to background γ rays (Bg), transitions in the photon flux monitor ^{27}Al [23], and to excitations in ^{48}Ti (container material), which are well known from previous NRF studies [25]. The spectra are dominated by strong excitations around 2.7–3.0 MeV marked by (1^+) , which are ascribed to $M1$ excitations to 1^+ mixed-symmetry states [27]. Candidates for $E1$ excitations [28] to the spin 1^- member of the $(2^+ \otimes 3^-)$ two-phonon quintuplet are labeled by (1^-) . The smooth energy variations of the 1^- two-phonon excitations and the $M1$ excitations to the 1^+ mixed-symmetry states are evident.

As previously discussed, in the case of even-even nuclei with a ground-state spin of $J_0 = 0$ unambiguous spin assignments to the excited states can be made from the intensities measured under scattering angles of 90° and 127° . As an example, in Fig. 3 the intensity ratios $W(90^\circ)/W(127^\circ)$ are plotted as a function of the excitation energy for the measurements on ^{124}Xe . The dashed and dotted lines correspond to the values \mathcal{D} and \mathcal{Q} expected for pure dipole and quadrupole excitations, respectively. Clearly, nearly all the Xe data points agree with the expectation value for dipole excitations. Therefore, for these photo-excited states in ^{124}Xe a spin of $J = 1$ can be assigned.

Figure 4 shows the obtained dipole strength distributions. Since no parity determination could be performed, the reduced ground-state transition widths $\Gamma_0^{\text{red}} = \Gamma_0/E_\gamma^3$ are plotted as a function of the excitation energy, which are proportional to the reduced excitation probabilities $B(E1) \uparrow$ and $B(M1) \uparrow$, respectively. For even-even nuclei a value of $\Gamma_0^{\text{red}} = 1 \text{ meV/MeV}^3$ corresponds to reduced excitation probabili-

ties of $B(E1) \uparrow = 2.866 \times 10^{-3} e^2\text{fm}^2$ or $B(M1) \uparrow = 0.259 \mu_N^2$, respectively. The strong excitations between 2.7 and 3.0 MeV marked by full circles are ascribed to $M1$ excitations to 1^+ mixed-symmetry states (see Sec. VB). Excitations in $^{134,132,130,128}\text{Xe}$ (labeled by open diamonds) are attributed to the $E1$ two-phonon excitations (see Sec. VA). In the $O(6)$ candidates $^{124,126}\text{Xe}$ rather strong low-lying dipole excitations emerge between 2.0 and 2.5 MeV; these may be due to the low-energy octupole strengths expected for these isotopes [29].

The results of the present experiments on the even-even isotopes $^{124,126,128,130,132,134,136}\text{Xe}$ are summarized in numerical form in Tables II–VIII. Given are the excitation energies E_x , total elastic scattering cross sections $I_{S,0}$, and the ground-state widths Γ_0 . Furthermore, the branching ratios $R_{\text{exp},1}$ and $R_{\text{exp},2}$ (assuming pure dipole transitions), if observed, for decays to the first or second excited 2^+ state are quoted, as are the reduced excitation strengths, both $B(M1) \uparrow$ and $B(E1) \uparrow$, since no parity assignments could be made.

Besides this huge number of dipole excitations, in addition, several electric quadrupole excitations could be observed in the even-even Xe isotopes. The results are summarized in Table IX. Given are the excitation energies E_x , the total elastic scattering intensities $I_{S,0}$, the spin and parity assignment J^π , the ground-state decay widths Γ_0 , and the reduced excitation probabilities $B(E2) \uparrow$. Safe spin assignments 2^+ are quoted if the intensity ratio $\mathcal{R} = W(90^\circ)/W(127^\circ)$ is more than three standard deviations (3σ) away from the dipole expectation value \mathcal{D} and within two σ in agreement with the quadrupole expectation value \mathcal{Q} . Tentative spin assignments $(2^+, 1)$ are given in cases where $\mathcal{R} \geq \sqrt{\mathcal{D} \cdot \mathcal{Q}}$.

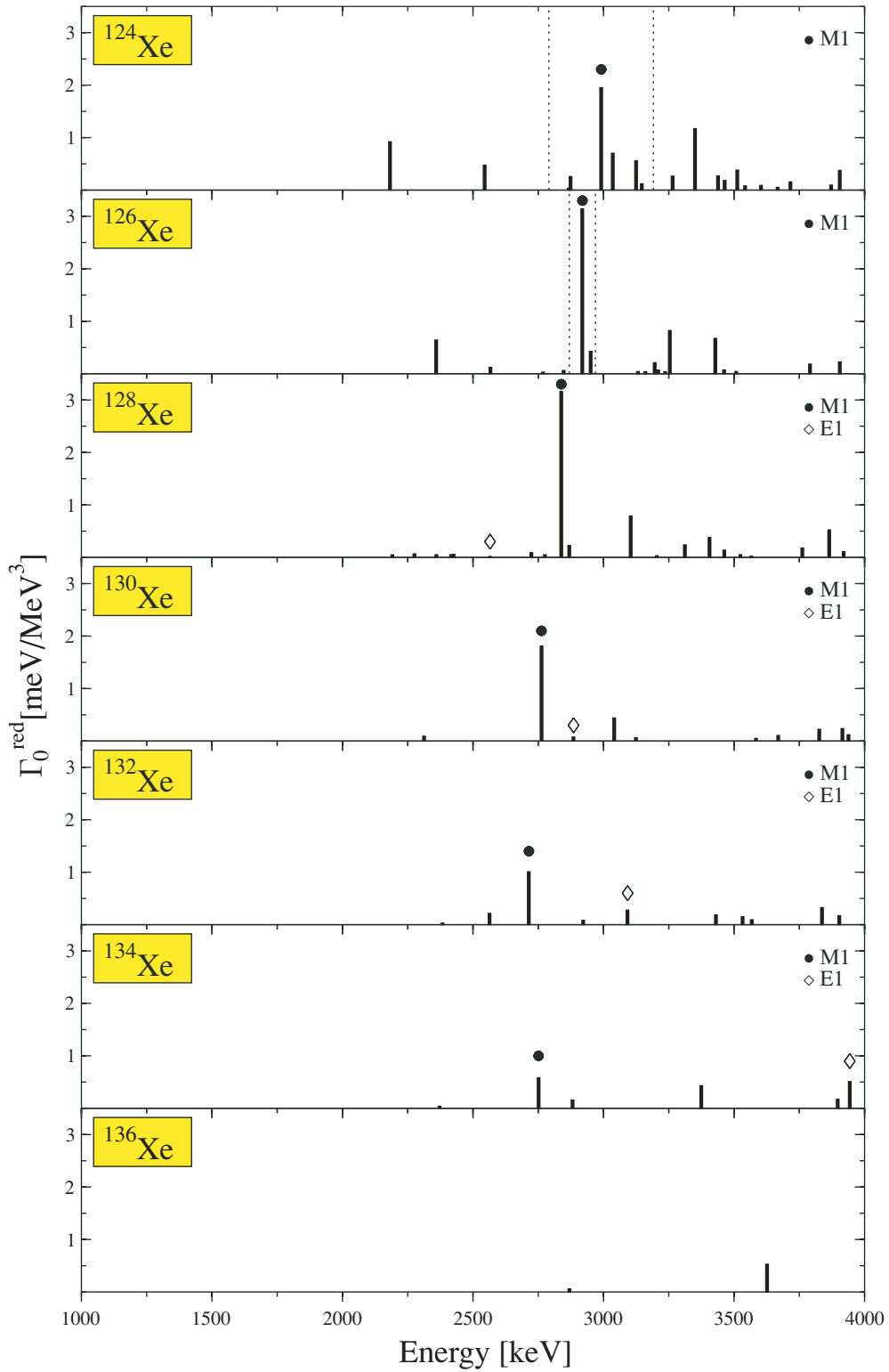


FIG. 4. (Color online) Systematics of dipole strength distributions in all stable even-even Xe isotopes $^{124-136}\text{Xe}$ observed in the present NRF experiments. Plotted are the reduced ground-state transition widths Γ_0^{red} as a function of the excitation energy. Candidates for the $E1$ two-phonon excitations are marked by open diamonds and those for $M1$ excitations to the 1^+ mixed-symmetry states by full circles. For further explanations see text.

TABLE II. Numerical results for dipole excitations in ^{124}Xe . The measured excitation energies E_x , the integrated cross sections $I_{S,0}$, and the branching ratios $R_{\text{exp},1,2}$ for the decays to the first and second 2^+ states, at 354.0 and 846.9 keV, respectively, are summarized. The ground-state transition widths Γ_0 and reduced excitation probabilities $B(M1) \uparrow$ and $B(E1) \uparrow$ were deduced.

E_x (keV)	$I_{S,0}$ (eV b)	$R_{\text{exp},1}$ $J_f^\pi = 2_1^+$	$R_{\text{exp},2}$ $J_f^\pi = 2_2^+$	Γ_0 (meV)	$B(M1) \uparrow$ (μ_N^2)	$B(E1) \uparrow$ ($10^{-3} e^2 \text{fm}^2$)
2182	18.7(13)	0.41(7)	—	9.6(6)	0.239(15)	2.64(17)
2545	5.9(5)	2.15(29)	—	7.8(6)	0.123(9)	1.36(10)
2867	1.1(3)	—	—	0.79(19)	0.009(2)	0.096(24)
2874	3.2(3)	2.42(35)	—	6.1(4)	0.067(5)	0.74(5)
2991	49.1(32)	0.34(3)	0.38(5)	52.2(26)	0.506(26)	5.59(28)
3036	21.0(14)	0.25(4)	—	19.6(12)	0.182(11)	2.01(12)
3125	16.6(12)	—	0.55(12)	17.1(12)	0.145(10)	1.60(11)
3147	1.1(2)	4.4(13)	—	3.7(5)	0.031(4)	0.34(5)
3265	1.9(4)	5.8(12)	—	9.2(8)	0.069(6)	0.76(7)
3350	45.2(30)	—	—	44.0(29)	0.303(20)	3.35(22)
3439	5.2(6)	1.44(23)	—	10.9(9)	0.069(6)	0.77(6)
3464	3.7(5)	1.34(25)	—	7.6(7)	0.048(4)	0.53(5)
3512	10.6(9)	0.31(7)	0.55(14)	16.5(13)	0.099(8)	1.09(8)
3542	3.3(5)	—	—	3.55(51)	0.021(3)	0.229(33)
3603	3.7(5)	—	—	4.17(58)	0.023(3)	0.256(36)
3667	2.2(5)	—	—	2.53(54)	0.013(3)	0.147(31)
3716	6.7(8)	—	—	8.01(94)	0.040(5)	0.447(52)
3872	4.2(10)	—	—	5.5(13)	0.025(6)	0.273(62)
3905	16.9(20)	—	—	22.3(26)	0.097(11)	1.08(13)

B. Results for the odd-mass isotopes $^{129,131}\text{Xe}$

Figure 5 shows the (γ, γ') spectra observed for the odd-mass isotopes $^{129,131}\text{Xe}$ in comparison with those of their even-even neighbors. A fragmentation of the dipole

strengths into weaker transitions in the odd-mass isotopes is evident. In Fig. 6 the dipole strength distributions observed in the odd-mass isotopes $^{129,131}\text{Xe}$ are compared with those in their even-even neighbor isotopes $^{128,130,132}\text{Xe}$. Since no

TABLE III. Numerical results for dipole excitations in ^{126}Xe . The measured excitation energies E_x , the integrated cross sections $I_{S,0}$, and the branching ratios $R_{\text{exp},1,2}$, at 388.6 and 879.9 keV, respectively, for the decays to the first and second 2^+ states are summarized. The ground-state transition widths Γ_0 and reduced excitation probabilities $B(M1) \uparrow$ and $B(E1) \uparrow$ were deduced.

E_x (keV)	$I_{S,0}$ (eV b)	$R_{\text{exp},1}$ $J_f^\pi = 2_1^+$	$R_{\text{exp},2}$ $J_f^\pi = 2_2^+$	Γ_0 (meV)	$B(M1) \uparrow$ (μ_N^2)	$B(E1) \uparrow$ ($10^{-3} e^2 \text{fm}^2$)
2359 ^a	9.4(7)	1.48(19)	—	8.4(5)	0.166(10)	1.84(12)
2567	1.6(5)	2.09(81)	—	2.1(4)	0.032(6)	0.35(7)
2768	0.9(3)	—	—	0.63(21)	0.008(3)	0.085(28)
2847	2.0(3)	—	—	1.42(21)	0.016(2)	0.176(26)
2919	78.5(51)	0.21(2)	0.61(7)	78.1(40)	0.815(41)	9.01(46)
2951	7.2(6)	1.53(23)	—	10.9(8)	0.110(8)	1.22(9)
3132	1.5(3)	—	—	1.24(24)	0.011(2)	0.116(22)
3160	1.3(3)	—	—	1.15(23)	0.009(2)	0.104(21)
3196	1.2(3)	7.9(21)	—	6.9(8)	0.054(6)	0.60(7)
3209	2.5(4)	—	—	2.27(31)	0.018(2)	0.197(27)
3236	1.4(3)	—	—	1.28(27)	0.010(2)	0.108(23)
3254	30.9(21)	—	—	28.4(19)	0.213(14)	2.36(16)
3428	20.0(14)	0.48(6)	—	27.2(16)	0.175(10)	1.94(12)
3462	1.9(4)	0.72(32)	—	3.0(6)	0.019(4)	0.21(4)
3508	1.7(4)	—	—	1.81(48)	0.011(3)	0.120(32)
3791	8.0(8)	—	—	10.0(11)	0.048(5)	0.527(55)
3905	4.7(9)	—	2.51(76)	13.4(21)	0.058(9)	0.64(10)

^aQuoted in the Nuclear Data Sheets [30] with a tentative spin assignment (2^+).

TABLE IV. Numerical results for dipole excitations in ^{128}Xe . The measured excitation energies E_x , the integrated cross sections $I_{S,0}$, and the branching ratios $R_{\text{exp},2}$, at 442.9 and 969.5 keV, respectively, for the decays to the first and second 2^+ states are summarized. The ground-state transition widths Γ_0 and reduced excitation probabilities $B(M1) \uparrow$ and $B(E1) \uparrow$ were deduced.

E_x (keV)	$I_{S,0}$ (eV b)	$R_{\text{exp},1}$ $J_f^\pi = 2_1^+$	$R_{\text{exp},2}$ $J_f^\pi = 2_2^+$	Γ_0 (meV)	$B(M1) \uparrow$ (μ_N^2)	$B(E1) \uparrow$ ($10^{-3} e^2 \text{fm}^2$)
2191	1.2(3)	—	—	0.52(11)	0.013(3)	0.141(29)
2276	1.7(3)	—	—	0.78(15)	0.017(3)	0.191(35)
2360	1.3(3)	—	—	0.65(14)	0.013(3)	0.142(31)
2416	1.4(3)	—	—	0.70(13)	0.013(2)	0.142(27)
2565	0.5(2)	—	—	0.29(11)	0.004(2)	0.049(18)
2724	2.8(3)	—	—	1.80(22)	0.023(3)	0.256(31)
2776	1.6(2)	—	—	1.04(16)	0.013(2)	0.139(22)
2838	76.1(49)	0.17(2)	0.90(10)	72.2(36)	0.819(41)	9.05(46)
3104	18.0(12)	0.89(10)	—	23.4(12)	0.203(11)	2.25(12)
3204	1.2(2)	—	—	1.03(22)	0.008(2)	0.090(19)
3312	1.8(3)	6.4(12)	—	8.6(7)	0.062(5)	0.68(5)
3406	6.9(6)	0.61(11)	2.11(34)	15.1(10)	0.099(7)	1.09(8)
3463	3.4(5)	0.95(22)	—	5.7(6)	0.036(4)	0.39(4)
3524	2.1(4)	—	—	2.26(47)	0.013(3)	0.148(31)
3566	0.9(3)	—	—	0.98(38)	0.006(2)	0.062(24)
3761	2.3(5)	—	5.8(15)	9.5(12)	0.046(6)	0.51(7)
3865	23.2(19)	—	—	30.1(24)	0.135(11)	1.50(12)
3920	4.8(12)	—	—	6.5(15)	0.028(7)	0.308(73)

spin assignments were possible, the products of the statistical spin factor g and the reduced transition width Γ_0^{red} are plotted as a function of the excitation energy. For the even-even isotopes the $E1$ excitations to the two-phonon states are marked by open diamonds, and the dominating $M1$ excitations to the 1^+ mixed-symmetry states are labeled by full dots. The dashed and dashed-dotted lines in the figures for the odd-mass isotopes represent summation limits of ± 300 and ± 500 keV around the strong $M1$ excitations in the even-even neighbors, respectively (see discussion). Obviously, the predominant $M1$ excitations to 1^+ mixed-symmetry states in the even-even isotopes are strongly fragmented in the odd-mass isotopes. The numerical

data for the odd-mass isotopes $^{129,131}\text{Xe}$ are summarized in Tables X and XI.

C. Comparison with previous work

Unfortunately, for the odd-mass isotopes $^{129,131}\text{Xe}$ no spin and parity assignments were possible from the present experiments. Therefore, and in view of the already high level density above about 2 MeV in these odd-mass nuclei, comparisons with existing data seem to be in appropriate and inconclusive.

TABLE V. Numerical results for dipole excitations in ^{130}Xe . The measured excitation energies E_x , the integrated cross sections $I_{S,0}$, and the branching ratios $R_{\text{exp},2}$ for the decays to the first and second 2^+ states, at 536.1 and 1122.2 keV, respectively, are summarized. The ground-state transition widths Γ_0 and reduced excitation probabilities $B(M1) \uparrow$ and $B(E1) \uparrow$ were deduced.

E_x (keV)	$I_{S,0}$ (eV b)	$R_{\text{exp},1}$ $J_f^\pi = 2_1^+$	$R_{\text{exp},2}$ $J_f^\pi = 2_2^+$	Γ_0 (meV)	$B(M1) \uparrow$ (μ_N^2)	$B(E1) \uparrow$ ($10^{-3} e^2 \text{fm}^2$)
2313	2.5(3)	—	—	1.14(16)	0.024(3)	0.264(36)
2763	41.5(27)	0.18(3)	1.40(19)	38.1(21)	0.469(25)	5.19(28)
2885	2.5(3)	—	—	1.84(24)	0.020(3)	0.219(28)
3041	15.4(11)	—	—	12.34(87)	0.114(8)	1.258(89)
3124	2.3(3)	—	—	1.92(29)	0.016(2)	0.180(27)
3584	2.1(4)	—	—	2.31(50)	0.013(3)	0.144(31)
3669	4.5(7)	—	—	5.22(82)	0.027(4)	0.303(48)
3826	9.8(12)	—	—	12.5(16)	0.058(7)	0.640(79)
3915	10.6(16)	—	—	14.1(21)	0.061(9)	0.68(10)
3938	5.4(17)	—	—	7.3(23)	0.031(10)	0.34(11)

TABLE VI. Numerical results for dipole excitations in ^{132}Xe . The measured excitation energies E_x , the integrated cross sections $I_{S,0}$, and the branching ratios $R_{\text{exp},1,2}$ for the decays to the first and second 2^+ states, at 667.7 and 1297.9 keV, respectively, are summarized. The ground-state transition widths Γ_0 and reduced excitation probabilities $B(M1) \uparrow$ and $B(E1) \uparrow$ were deduced.

E_x (keV)	$I_{S,0}$ (eV b)	$R_{\text{exp},1}$ $J_f^\pi = 2_1^+$	$R_{\text{exp},2}$ $J_f^\pi = 2_2^+$	Γ_0 (meV)	$B(M1) \uparrow$ (μ_N^2)	$B(E1) \uparrow$ ($10^{-3} e^2 \text{fm}^2$)
2383	0.8(2)	—	—	0.40(12)	0.008(2)	0.085(25)
2563	2.5(3)	3.94(81)	—	3.6(4)	0.056(6)	0.61(7)
2714	24.4(20)	—	2.07(49)	20.1(16)	0.261(21)	2.89(23)
2922	2.8(4)	—	—	2.08(26)	0.022(3)	0.239(30)
3092	6.7(5)	1.00(18)	—	8.2(6)	0.072(5)	0.80(6)
3431	7.3(6)	—	—	7.46(65)	0.048(4)	0.529(46)
3533	6.1(6)	—	—	6.63(65)	0.039(4)	0.431(42)
3568	1.2(3)	3.9(12)	—	4.2(7)	0.024(4)	0.27(4)
3837	14.3(14)	—	—	18.3(18)	0.084(8)	0.930(89)
3903	7.7(11)	—	—	10.2(15)	0.044(6)	0.490(72)

Comprehensive data exist for the stable even-even Xe isotopes, mainly on positive parity states and collective excitations. However, practically no information has been available up to now on low-lying spin 1 levels. None of the numerous dipole excitations to spin 1 states in $^{124,126,128,130,132,134,136}\text{Xe}$, observed in the present NRF experiments, had been previously known. Therefore, the following comparison is restricted to the observed candidates of 2^+ states (see Table IX), which are only weakly excited in the present photon scattering studies. Most of them were previously unknown; the exceptions are summarized in the following.

1. ^{124}Xe

No excitations of low-lying 2^+ states could be detected in the present work.

2. ^{126}Xe

The state at 2228 keV with a tentative spin assignment (2^+ , 1), observed in the present NRF experiments, is known from γ spectroscopic studies of transitions in ^{126}Xe following the β decay of ^{126}Cs [34]. From these results the spin of the level was restricted to values of 0^+ , 1, or 2. A level at

2359 keV was reported recently by Gade *et al.* [35], based on γ spectroscopic studies in a comprehensive investigation of low-lying collective excitations in ^{126}Xe via the $^{123}\text{Te}(\alpha, n)$ reaction. From these experiments a tentative spin of (2^+) was assigned to this level. Furthermore, an upper limit for the lifetime of $\tau \leq 70(30)$ fs could be given from Doppler shift attenuation measurements. In the present NRF experiments a state at 2359 keV was found too; however, the angular distribution measurements clearly favor a spin of 1. However, the lifetime of $\tau = 42(7)$ fs, deduced from the measured scattering cross section and decay branching, corresponds to that reported by Gade *et al.* [35].

3. ^{128}Xe

A 2^+ state at 2837.6 keV, exhibiting a very strong decay branch to the first 2^+ state at 443 keV, was reported from γ spectroscopic investigations of transitions in ^{128}Xe following the β decay of ^{128}Cs [36,37]. In the present NRF study a level at 2838 keV was observed too, however, with a clear spin 1 signature and a different decay pattern (a strong decay to the second 2^+ state at 969.5 keV). Therefore, a correspondence of both levels seems to be questionable.

TABLE VII. Numerical results for dipole excitations in ^{134}Xe . The measured excitation energies E_x , the integrated cross sections $I_{S,0}$, and the branching ratios $R_{\text{exp},1,2}$ for the decays to the first and second 2^+ states, at 847.0 and 1613.8 keV, respectively, are summarized. The ground-state transition widths Γ_0 and reduced excitation probabilities $B(M1) \uparrow$ and $B(E1) \uparrow$ were deduced.

E_x (keV)	$I_{S,0}$ (eV b)	$R_{\text{exp},1}$ $J_f^\pi = 2_1^+$	$R_{\text{exp},2}$ $J_f^\pi = 2_2^+$	Γ_0 (meV)	$B(M1) \uparrow$ (μ_N^2)	$B(E1) \uparrow$ ($10^{-3} e^2 \text{fm}^2$)
2372	1.1(3)	—	—	0.54(13)	0.011(2)	0.116(28)
2751	18.4(13)	—	—	12.10(84)	0.151(10)	1.67(12)
2881	1.9(3)	4.9(14)	—	3.8(6)	0.041(7)	0.45(8)
3374	16.8(12)	—	—	16.6(12)	0.112(8)	1.235(88)
3897	7.6(11)	—	—	10.0(15)	0.044(6)	0.486(71)
3943	23.1(24)	—	—	31.2(32)	0.132(14)	1.46(15)

TABLE VIII. Numerical results for dipole excitations in ^{136}Xe . The measured excitation energies E_x , the integrated cross sections $I_{S,0}$, and the branching ratios $R_{\text{exp},1,2}$ for the decays to the first and second 2^+ states, at 1313.0 and 2289.5 keV, respectively, are summarized. The ground-state transition widths Γ_0 and reduced excitation probabilities $B(M1) \uparrow$ and $B(E1) \uparrow$ were deduced.

E_x (keV)	$I_{S,0}$ (eV b)	$R_{\text{exp},1}$ $J_f^\pi = 2_1^+$	$R_{\text{exp},2}$ $J_f^\pi = 2_2^+$	Γ_0 (meV)	$B(M1) \uparrow$ (μ_N^2)	$B(E1) \uparrow$ ($10^{-3} e^2 \text{fm}^2$)
2869 ^a	1.9(3)	—	—	1.39(19)	0.015(2)	0.169(23)
3626	12.3(10)	3.08(49)	—	25.2(19)	0.137(10)	1.52(12)

^aAn $E2$ character cannot be excluded.

4. ^{130}Xe

The 2^+ state at 1122.1 keV is known from diverse β -decay-, γ -spectroscopic, and reaction studies (see, e.g. compilation in Ref. [31]). An upper limit of the half-life of $t_{1/2} \leq 3$ ns is quoted [31] in agreement with the present findings of a ground-state decay width of $\Gamma_0 = 0.25(8)$ meV corresponding to $t_{1/2} = 1.8(6)$ ps.

5. ^{132}Xe

States with tentative spin assignments ($1, 2^+$) at 2168.8 and 2714.4 keV are known from (n, γ) [38,39] and ($d, ^3\text{He}$)-

reaction studies [40]. In the present NRF work a corresponding state at 2714 keV, however, with a clear spin 1 assignment, was observed. Near 2169 keV no excitations could be detected.

6. ^{134}Xe

The low-lying 2^+ state at 1614 keV is established from β -decay and γ spectroscopic investigations [41,42].

7. ^{136}Xe

The low-lying 2^+ level at 1331 keV is known from diverse investigations (see, e.g., the compilation of Ref. [33]). Its quoted half life of $t_{1/2} = 0.36$ ps is in crude agreement with the findings of the present NRF work [$\Gamma_0 = 0.83(12)$ meV, corresponding to $t_{1/2} = 0.55(8)$ ps]. The 2^+ levels at 2289 and 2415 keV were already reported from γ spectroscopy of separated fission fragments [43]. A state at 2869 keV with tentative spin assignments ($1, 2$) or $2^{(+)}$ quoted in Refs. [43] and [33] may correspond to the 2869 keV excitation observed in the present experiments. However, here a spin of 1 is favored, even if a spin of 2^+ cannot be excluded definitely.

V. DISCUSSION

A. $E1$ two-phonon excitations in the even-even isotopes $^{124-136}\text{Xe}$

The lowest excited states in even-even nuclei near closed neutron or proton shells are usually $J^\pi = 2^+$ and $J^\pi = 3^-$ levels originating from quadrupole or octupole vibrations of the nuclear shape. In a simple collective picture one expects the coupling of the corresponding single phonons to two-phonon or even multiphonon excitations. Of particular interest are couplings of different phonons. In these cases rather pure multiphonon states and small anharmonicities are expected owing to the lack of Pauli blocking effects in the formation of the multiphonon wave functions. The simplest known examples of such an inhomogeneous phonon coupling are quadrupole-octupole two-phonon excitations $2^+ \otimes 3^-$, leading to a multiplet consisting of five states with spins and parities $J^\pi = 1^-, \dots, 5^-$.

Complete quadrupole-octupole quintuplets were first observed in nuclei near the $N = 82$ shell closure [44,45], but these have been established recently also in nuclei near the $Z = 50$ shell closure, the Cd isotopes ^{108}Cd [46], ^{112}Cd [47],

TABLE IX. Numerical results for candidates of electric quadrupole excitations observed in the even-even Xe isotopes. Given are the excitation energies E_x , the total elastic scattering intensities $I_{S,0}$, the assigned spins and parities J^π , the ground-state transition widths Γ_0 , and the reduced excitation probabilities $B(E2) \uparrow$. The criteria for the spin assignments are explained in the text.

Isotope	E_x (keV)	$I_{S,0}$ (eV b)	J^π (\hbar)	Γ_0 (meV)	$B(E2) \uparrow$ ($e^2 \text{fm}^4$)
^{124}Xe	—	—	—	—	—
^{126}Xe	2228	1.7(4)	($2^+, 1$)	0.44(16)	50(11)
^{128}Xe	—	—	—	—	—
^{130}Xe	1121 ^a	3.7(7)	2^+	0.25(8)	860(167)
	2030	2.0(4)	($2^+, 1$)	0.44(14)	79(15)
	2162	1.3(4)	($2^+, 1$)	0.32(14)	42(11)
	2345	1.2(3)	($2^+, 1$)	0.35(13)	31(7)
	2523	0.8(2)	($2^+, 1$)	0.27(13)	16(5)
	3530	2.0(5)	($2^+, 1$)	1.28(52)	14(4)
	3596	1.2(4)	($2^+, 1$)	0.84(44)	9(3)
^{132}Xe	1761	1.6(4)	($2^+, 1$)	0.26(11)	98(25)
	2929	1.4(3)	($2^+, 1$)	0.61(22)	17(4)
	3113	0.9(2)	($2^+, 1$)	0.46(18)	10(2)
^{134}Xe	1614 ^b	1.8(4)	($2^+, 1$)	0.25(9)	141(32)
	2262	1.4(3)	($2^+, 1$)	0.38(12)	40(8)
	3493	2.5(4)	2^+	1.58(38)	19(3)
	3542	1.9(4)	($2^+, 1$)	1.25(38)	14(3)
^{136}Xe	1313 ^c	9.2(8)	2^+	0.83(12)	1323(117)
	2289 ^c	1.6(3)	($2^+, 1$)	0.45(13)	45(8)
	2415 ^c	4.3(4)	2^+	1.31(21)	100(10)
	3350	2.2(4)	($2^+, 1$)	1.29(34)	19(3)
	3675	7.4(7)	2^+	5.17(85)	48(5)

^aQuoted in the Nuclear Data Sheets [31] as a 2^+ level.

^bQuoted in the Nuclear Data Sheets [32] as a 2^+ level.

^cQuoted in the Nuclear Data Sheets [33] as a 2^+ level.

TABLE X. Results for dipole excitations in ^{129}Xe . Excitation energies E_x , total elastic scattering cross sections $I_{S,0}$, the product of the statistical factor g times the ground-state widths Γ_0 , the branching ratio $R_{\text{exp},i}$ to low-lying excited states, the reduced ground-state widths Γ_0^{red} , and the reduced excitation strengths, $B(M1) \uparrow$ and $B(E1) \uparrow$, are given.

E_x (keV)	$I_{S,0}$ (eV b)	$g \cdot \Gamma_0$ (meV)	$R_{\text{exp},i}$	$g \cdot \Gamma_0^{\text{red}}$ (meV/MeV ³)	$B(M1) \uparrow$ (μ_N^2)	$B(E1) \uparrow$ ($10^{-3} e^2 \text{fm}^2$)
1239	2.0(4)	0.82(18)	—	0.43(9)	0.111(24)	1.23(27)
1570	5.4(5)	3.44(34)	—	0.89(9)	0.230(23)	2.55(26)
1884	1.4(3)	1.33(29)	—	0.20(4)	0.052(11)	0.57(12)
2186	0.8(2)	1.06(26)	—	0.10(2)	0.026(6)	0.291(70)
2289	1.4(3)	1.86(37)	—	0.15(3)	0.040(8)	0.444(88)
2343	4.1(4)	5.82(56)	—	0.45(4)	0.117(11)	1.30(13)
2355	6.4(5)	9.22(71)	—	0.71(5)	0.183(14)	2.03(16)
2383	1.5(2)	2.17(37)	—	0.16(3)	0.042(7)	0.459(79)
2394	4.9(5)	7.36(69)	—	0.54(5)	0.139(13)	1.54(14)
2425	2.0(3)	6.31(88)	1.98(55) ^a	0.44(6)	0.115(16)	1.268(18)
2499	2.5(3)	4.03(44)	—	0.26(3)	0.067(7)	0.740(80)
2554	1.3(2)	2.22(36)	—	0.13(2)	0.035(6)	0.382(61)
2592	3.0(3)	5.25(52)	—	0.30(3)	0.078(8)	0.864(85)
2674	1.2(2)	2.24(36)	—	0.12(2)	0.030(5)	0.335(54)
2724	1.2(2)	2.25(44)	—	0.11(2)	0.029(6)	0.320(63)
2744	0.7(2)	6.3(11)	9.0(29) ^b	0.30(5)	0.079(14)	0.874(16)
2767	1.1(3)	2.15(51)	—	0.10(2)	0.026(6)	0.291(69)
2776	1.2(2)	2.51(41)	—	0.12(2)	0.030(5)	0.337(55)
2793	2.3(3)	4.67(53)	—	0.21(2)	0.056(6)	0.615(70)
2854	1.7(2)	3.62(46)	—	0.16(2)	0.040(5)	0.446(57)
2917	0.7(2)	1.46(36)	—	0.06(2)	0.015(4)	0.169(42)
2972	0.9(2)	2.17(45)	—	0.08(2)	0.021(4)	0.237(49)
3015	0.9(2)	2.20(44)	—	0.08(2)	0.021(4)	0.230(45)
3023	0.8(2)	1.96(51)	—	0.07(2)	0.018(5)	0.203(53)
3215	1.7(3)	4.60(85)	—	0.14(3)	0.036(7)	0.397(74)
3783	1.2(4)	4.5(13)	—	0.08(2)	0.021(6)	0.237(71)
3805	1.2(3)	4.6(13)	—	0.08(2)	0.021(6)	0.238(66)
3829	1.2(4)	4.5(14)	—	0.08(3)	0.021(7)	0.230(74)

^aDecay to the excited state at 442 keV ($J^\pi = (5/2)^+$).

^bDecay to the excited state at 693 keV ($J^\pi = (3/2, 5/2)$).

TABLE XI. Results for dipole excitations in ^{131}Xe . Excitation energies E_x , total elastic scattering cross sections $I_{S,0}$, the product of the statistical factor g times the ground-state widths Γ_0 , the branching ratio R_{exp} to the excited state at 565 keV, the reduced ground-state widths Γ_0^{red} , and the reduced excitation strengths, $B(M1) \uparrow$ and $B(E1) \uparrow$ are given.

E_x (keV)	$I_{S,0}$ (eV b)	$g \cdot \Gamma_0$ (meV)	$R_{\text{exp},1}$	$g \cdot \Gamma_0^{\text{red}}$ (meV/MeV ³)	$B(M1) \uparrow$ (μ_N^2)	$B(E1) \uparrow$ ($10^{-3} e^2 \text{fm}^2$)
1665	2.7 (7)	1.93(52)	—	0.42(11)	0.108(29)	1.20(32)
2007	2.1 (5)	2.21(50)	—	0.27(6)	0.071(16)	0.78(18)
2359	0.7 (4)	1.00(54)	—	0.08(4)	0.020(11)	0.22(12)
2378	2.3 (3)	3.41(49)	—	0.25(4)	0.066(9)	0.73(10)
2396	1.1 (3)	1.57(45)	—	0.11(3)	0.030(8)	0.328(94)
2570	1.3 (3)	2.30(47)	—	0.14(3)	0.035(7)	0.388(80)
2601	1.5 (3)	2.65(51)	—	0.15(3)	0.039(8)	0.431(83)
2662	1.2 (2)	2.14(45)	—	0.11(2)	0.029(6)	0.326(68)
2675	1.4 (3)	2.62(52)	—	0.14(3)	0.035(7)	0.392(78)
2833	1.5 (3)	3.17(59)	—	0.14(3)	0.036(7)	0.400(75)
2848	3.0 (5)	6.3(10)	—	0.27(4)	0.071(12)	0.78(13)
2852	2.0 (4)	4.24(91)	—	0.18(4)	0.047(10)	0.52(11)
3088	1.0 (3)	11.5(15)	6.6 (20)	0.39(5)	0.101(13)	1.120(15)
3126	1.5 (3)	3.93(75)	—	0.13(2)	0.033(6)	0.368(71)
3175	1.0 (3)	2.65(74)	—	0.08(2)	0.021(6)	0.237(66)

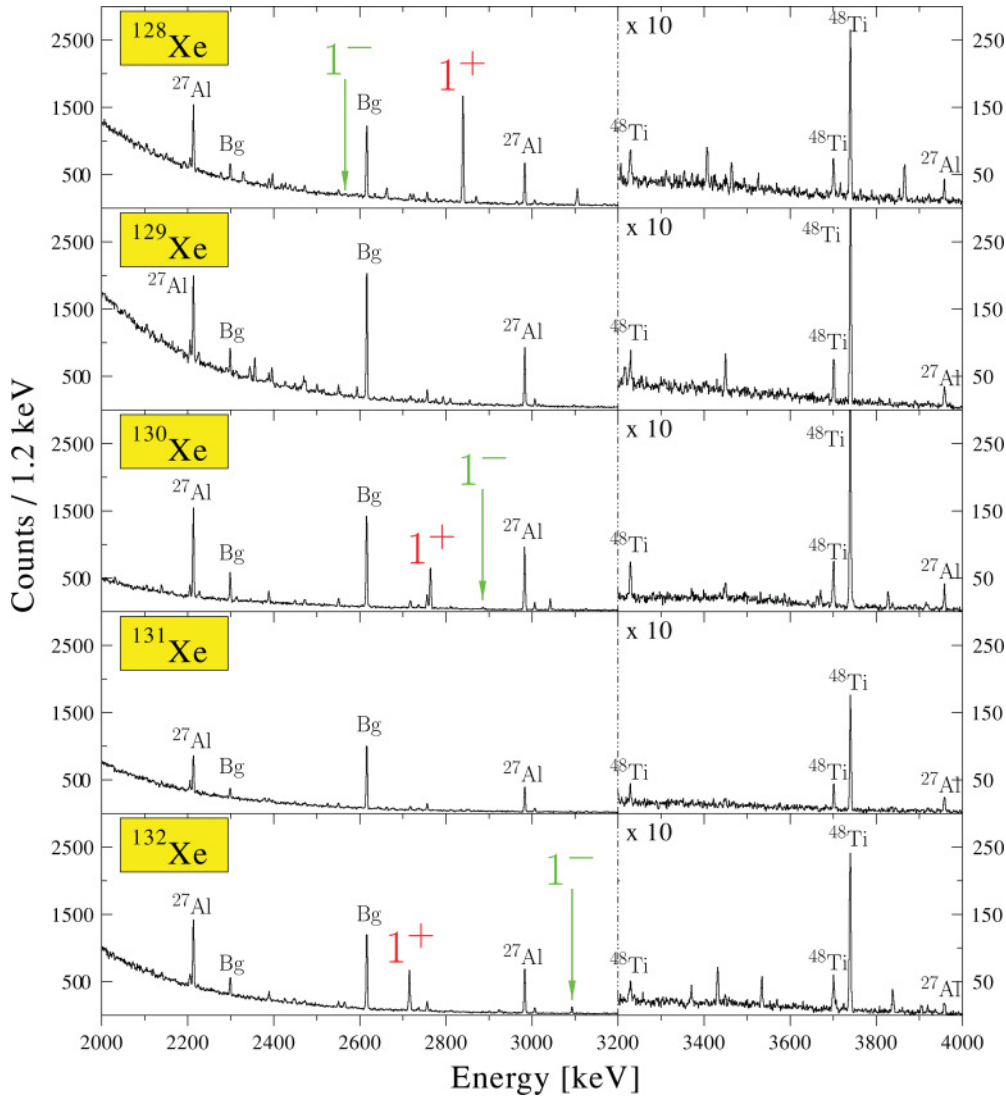


FIG. 5. (Color online) (γ , γ') spectra observed for stable odd-mass isotopes $^{129,131}\text{Xe}$ in comparison with those of their even-even neighbor isotopes. For further explanations see caption of Fig. 2.

and ^{114}Cd [48], and ^{112}Sn [49]. The properties of this negative parity quintuplet were calculated already in 1971 by Vogel and Kocbach [50].

In photon scattering experiments the 1^- member of the $2^+ \otimes 3^-$ multiplet can be excited selectively by an $E1$ transition from the ground state. A common feature of these $E1$ excitations, which were observed as a general phenomenon in nuclei near the shell closures $Z, N = 28; Z, N = 50; N = 82$ [28] are excitation energies E_{1^-} very close to the sum ($E_{2^+} + E_{3^-}$) of the corresponding one-phonon energies, suggesting a nearly harmonic coupling. The two-phonon nature of these 1^- states has been confirmed by measurements of the branching ratios of their one-phonon decays into the 3_1^- and 2_1^+ vibrational states [51,52]. A comprehensive compilation of existing experimental NRF data and their interpretation can be found in Ref. [28].

The observed excitation strengths $B(E1) \uparrow$ vary only smoothly in magic nuclei. In the tin isotopes $^{116,118,120,122,124}\text{Sn}$

($Z = 50$) [53] and ^{112}Sn [54] and in the neighboring Cd ($Z = 48$) (see Ref. [55]) and Te ($Z = 52$) isotopes [56,57] the observed transition strengths smoothly increase with lower neutron numbers. Analogously, the excitation strengths in the $N = 82$ isotones also exhibit a slight decrease with lowered proton numbers. However, the excitation strengths are steeply reduced when moving away from the shell closure (see Ref. [28]).

An outstanding case to study this behavior in detail represents the long chain of stable Xe isotopes. The data for the ascribed two-phonon excitations in the even-even Xe isotopes are summarized in Fig. 7. Their excitation energies are shown in the upper part by full circles. Obviously, they lie nearly at the sum energy $\Sigma = E_{2^+} + E_{3^-}$ of the corresponding one-phonon excitations, documenting a rather harmonic coupling. In the lower part of the figure the $B(E1) \uparrow$ values are depicted. A steep decrease of the strengths is observed when moving away from the closed shell $N = 82$. The same

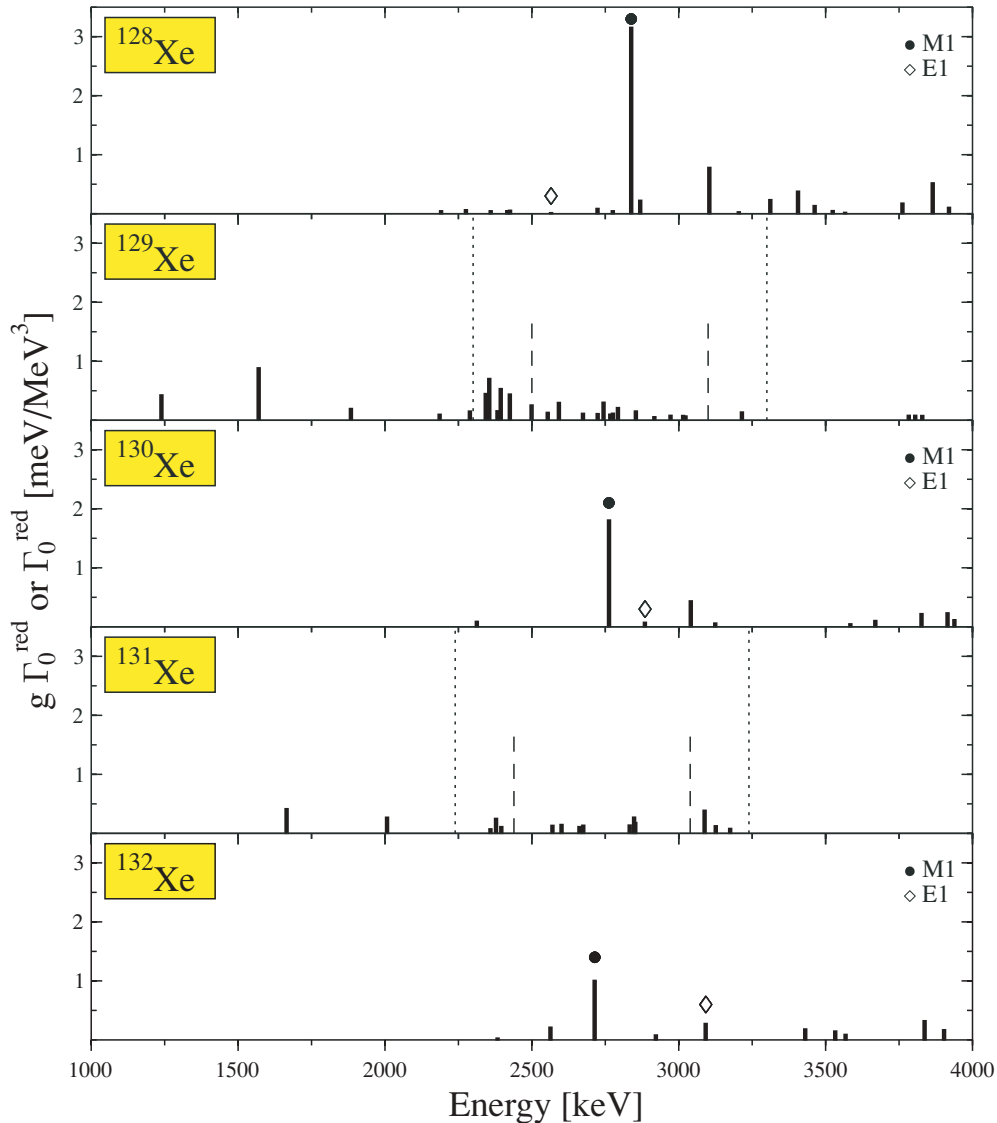


FIG. 6. (Color online) Systematics of dipole strength distributions in the odd-mass isotopes $^{129,131}\text{Xe}$ in comparison with those in their even-even neighbor isotopes. For further explanations see caption of Fig. 4.

behavior was seen in recent Stuttgart NRF experiments on the neighboring Ba isotopes [58]. The two-phonon excitations were observed only in $^{128,130,132,134}\text{Xe}$. For $^{124,126}\text{Xe}$ the experimental sensitivity obviously was not sufficient. For the magic isotope ^{136}Xe ($N = 82$) the excitation is expected at about 4.6 MeV, an energy that was not accessible at the Stuttgart facility. The numerical data for the candidates of the two-phonon excitations are summarized in Table XII.

In Fig. 8 the reduced transition probabilities $B(E1, 1 \rightarrow 0)$ for the two-phonon excitations in all nuclei near the $N = 82$ shell closures, studied in photon scattering experiments, are summarized. The $B(E1, 1 \rightarrow 0)$ values are plotted as a function of the neutron and proton numbers, respectively. The results observed for the Xe isotopes are shown by full bars. The new Xe data fit nicely into this systematic of the two-phonon excitations in nuclei near the $N = 82$ shell closure. Obviously, the strengths are highest for magic nuclei and drop steeply

when moving away from the shell closure marked by the bold line at $N = 82$. Such a behavior was observed at all shell closures and can be explained by the dipole core polarization effect, arising from mixings with the electric GDR (see Ref. [28]), and is supported by calculations in the framework of the quasiparticle-phonon-model (QPM) [59,60]. Jolos and Scheid [61] provided another successful description of the enhanced electric dipole transitions in nuclei near shell closures with strong collective correlations in the framework of a model based on cluster-type correlations. A satisfactory explanation of the properties of low-lying 1^- states in spherical nuclei and their decay characteristics can also be given within the Q -phonon scheme [62].

Quite recently, Jolos and co-workers studied the neutron number dependence of the reduced transition probabilities $B(E1)$ in spherical nuclei within the Q -phonon approach in the fermionic space [63]. A good description of the experimental

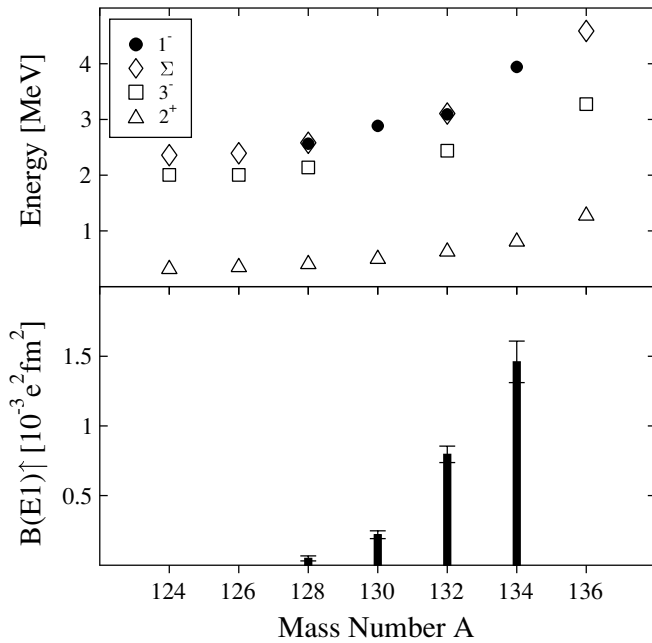


FIG. 7. Systematics of $E1$ two-phonon excitations in the even-even Xe isotopes. Upper part: Energies of the 2_1^+ (open triangles) and 3_1^- (open squares) one-phonon excitations and of the observed 1^- two-phonon excitations (full circles) in $^{124-136}\text{Xe}$ compared to the expected sum energies $\Sigma = E_{2^+} + E_{3^-}$ (open diamonds). Lower part: Experimental $B(E1) \uparrow$ values for the two-phonon excitations (full symbols). Error bars are smaller than the symbol sizes if not explicitly depicted.

data was achieved. In particular, for the Xe isotopes the steep decrease of the $E1$ strengths, when moving away from the $N = 82$ shell closure with a minimum for ^{128}Xe , is well explained. However, the predicted increase of the strengths in $^{126,124}\text{Xe}$ cannot be confirmed unambiguously by the present experimental data. In both isotopes strong dipole excitations were detected at low energies (see Fig. 4). However, their energies or decay characteristics do not correspond to the

TABLE XII. $E1$ two-phonon excitations in the even- A stable Xe isotopes ($Z = 54$). Given are the experimentally observed excitation energies E_{1^-} of the 1^- levels of the two-phonon quintuplet ($2^+ \otimes 3^-$) together with the energies of the corresponding one-phonon excitations E_{2^+} and E_{3^-} and their sums ($E_{2^+} + E_{3^-}$). In addition, excitation strengths $B(E1) \uparrow$ are reported. The question marks represent values unknown from the literature. Dashes indicate excitations undetected in the present experiments.

Isotope	E_{1^-} (keV)	E_{2^+} (keV)	E_{3^-} (keV)	$(E_{2^+} + E_{3^-})$ (keV)	$B(E1) \uparrow$ ($10^{-3} e^2 \text{ fm}^2$)
^{124}Xe	—	354.1	2005	2359.1	(≤ 0.05)
^{126}Xe	—	388.6	2004.9	2393.5	(≤ 0.06)
^{128}Xe	2565	442.9	2138.7	2581.6	0.049(18)
^{130}Xe	2885	536.1	?	?	0.219(28)
^{132}Xe	3092	667.7	2439.1	3106.2	0.796(59)
^{134}Xe	3943	847.0	?	?	1.46 (15)
^{136}Xe	—	1313	3275.2	4588.2	—

expected properties of the 1^- two-phonon states. Furthermore, $E1$ excitations should occur in this energy range because of the octupole strengths expected in these isotopes [29]. Therefore, more spectroscopic information, including safe parity determination, is needed to draw definite conclusions.

B. $M1$ excitations to 1^+ mixed-symmetry states in the even-even isotopes $^{124-136}\text{Xe}$

In addition to the $E1$ two-phonon excitations previously discussed, another general low-lying dipole mode in nuclei near shell closures consists of $M1$ excitations to so-called mixed-symmetry (MS) 1^+ states. Mixed-symmetry states are predicted in the interacting boson model IBM-2 and are not fully symmetric with respect to the proton-neutron degree of freedom [64–67]. The 1^+ MS states represent another example for an inhomogeneous coupling of two different vibrational phonons. They result from the coupling (in the valence space of heavy nuclei) of the isoscalar quadrupole excitation and the proton-neutron mixed-symmetry quadrupole excitation ($2_1^+ \otimes 2_{1,\text{ms}}^+$) [68]. A clear signature for the 1^+ MS states, accessible in photon scattering experiments, is the $M1$ decay branches to the ground state and to the 0_2^+ and 2_2^+ p - n symmetric two-phonon states.

A prominent example of $M1$ excitations to 1^+ MS states in deformed nuclei is the well-established *scissors mode*. After its prediction [69] and subsequent experimental discovery [70] this fundamental dipole mode was systematically studied in numerous electron [71] and photon scattering experiments [15] and rather complete systematics have been established [72–74]. However, for nearly spherical nuclei near shell closures little information on the MS 1^+ states is available. A nearly complete multiphonon MS multiplet was observed recently in ^{94}Mo [27,75], and other MS state structures have been seen mainly in nuclei around $N = 50$ [76–78]. In the mass region around the $N = 82$ shell closure from photon scattering experiments some results were reported on $2_{1,\text{ms}}^+$ states in ^{136}Ba [18] and ^{144}Sm [79]. Therefore, it was of interest to study the excitations to 1^+ MS states in the stable even-even nuclei of the long Xe isotopic chain, in particular to investigate the influence of the expected phase transition.

The dipole strength distributions in the even Xe isotopes are dominated by single strong excitations in the energy range between 2.7 and 3.0 MeV, which we ascribe to $M1$ excitations to 1^+ MS states (see Fig. 4). Figure 9 shows the excitation energies (upper part) and $B(M1) \uparrow$ values (lower part) of these excitations. The energies vary only smoothly between 2.7 and 3.0 MeV. The total strengths increase when moving from the closed shell nucleus ^{136}Xe to the O(6) candidates $^{126,124}\text{Xe}$, where the full strength was observed, as predicted within the O(6) limit [67]. These expectation values are shown in Fig. 9 as a dashed line. The numerical data are summarized in Table XIII.

Even if no direct parity determinations were possible, this interpretation is on rather safe grounds. First, the excitation energies and strengths are as expected from the systematics [72–74]. Furthermore, these states show strong decay branchings to the second 2_2^+ state with mostly symmetric two-phonon

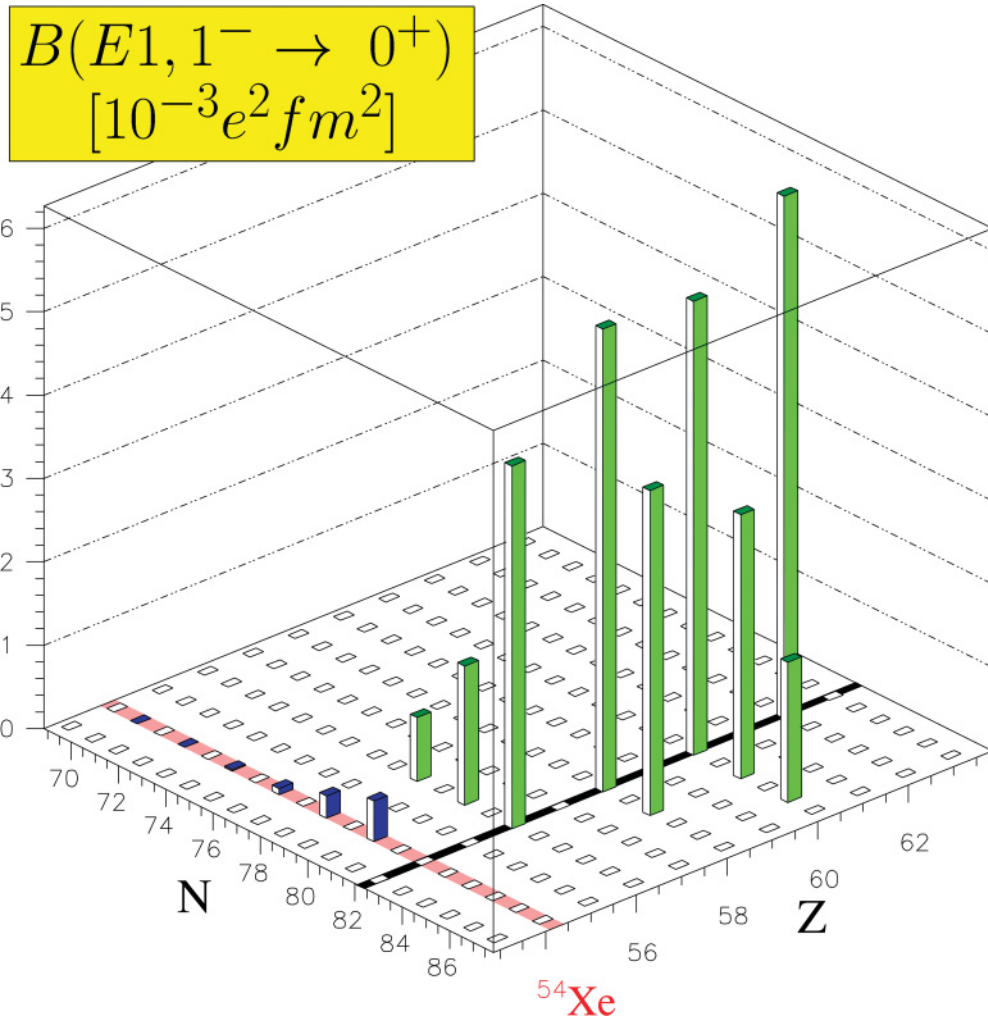


FIG. 8. (Color online) Reduced transition probabilities $B(E1, 1^- \rightarrow 0^+) = \frac{1}{3}B(E1, 0^+ \rightarrow 1^-)$ for $E1$ ground-state transitions of the two-phonon 1^- states in spherical nuclei near the $N = 82$ shell closure, marked by the bold line. Data are from the recent compilation of Ref. [28], supplemented by the present new Xe data (shown on the gray line).

TABLE XIII. The $B(M1) \uparrow$ values for candidates of 1^+ MS states experimentally observed in the even isotopes $^{124-136}\text{Xe}$ in comparison with predictions of the IBM-2 model in the $O(6)$ limit (see text).

Isotope	Energy (keV)	$B(M1) \uparrow$ (exp.) (μ_N^2)	$B(M1) \uparrow$ (theor.) (μ_N^2)
124	2991	0.940(66) ^a	0.955
126	2919	0.925(49) ^b	0.895
128	2838	0.819(41)	0.819
130	2763	0.469(25)	0.716
132	2714	0.261(21)	0.573
134	2751	0.151(11)	0.358
136	?	?	0

^aStrength summed in the energy interval ± 200 keV around the 2991 keV state.

^bStrength summed in the energy interval ± 50 keV around the 2919 keV state.

properties, a characteristic for the 1^+ MS states [27]. In Fig. 10 the decay branchings of the candidates for 1^+ MS states in the even-even Xe isotopes are depicted. The upper and lower parts show the branching ratios $R_{\text{exp},1}$ and $R_{\text{exp},2}$, respectively, defined for the MS 1^+ states as

$$R_{\text{exp},1} = \frac{B(E2, 1_{\text{ms}}^+ \rightarrow 2_1^+)}{B(M1, 1_{\text{ms}}^+ \rightarrow 0_1^+)}, \quad (7)$$

$$R_{\text{exp},2} = \frac{B(M1, 1_{\text{ms}}^+ \rightarrow 2_2^+)}{B(M1, 1_{\text{ms}}^+ \rightarrow 0_1^+)}. \quad (8)$$

Here pure $E2$ and $M1$ transitions were assumed for the decays to the 2_1^+ and 2_2^+ states, respectively, as characteristic for the decay of 1^+ MS states [67]. The experimental data (open symbols) are compared with IBM-2 predictions [67] shown as full or dotted lines. For these theoretical estimates bare $g_\pi = 1$ and $g_\nu = 0$ and effective charges $e_\pi = 0.22 e$ and $e_\nu = 0.06 e$, as obtained for the neighboring

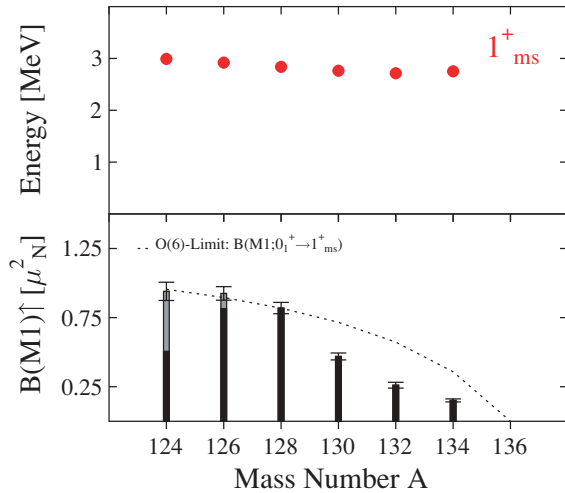


FIG. 9. (Color online) Systematics of the candidates for $M1$ excitations to mixed-symmetry 1^+ states in the even-even Xe isotopes as a function of the mass number A . Upper part: Excitation energies. Lower part: $B(M1) \uparrow$ excitation strengths. The dotted line gives the strengths predicted by IBM-2 in the O(6) limit. The gray areas in the bars for $^{124,126}\text{Xe}$ represent the summed strengths of the fragments of the $M1$ excitations. For further explanations see text.

nucleus ^{134}Ba [17], were used. At least the tendency of the experimental data is in qualitative agreement with the IBM-2 predictions in the O(6) limit.

A further independent support for the interpretation of these strong excitations as transitions to 1^+ MS states is the observation that their strengths scale linearly with β_2^2 , the square of the deformation parameter, which is proportional to the $B(E2)$ value. This so-called β_2^2 or δ^2 law (when using an alternative definition of a deformation parameter) was first experimentally observed in the Sm [80,81] and Nd [13,14]

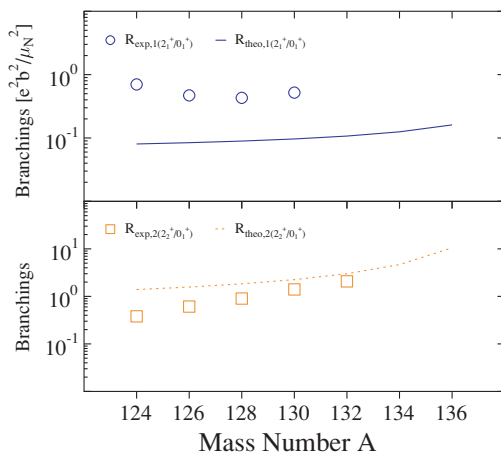


FIG. 10. (Color online) Decay branchings of the candidates for mixed-symmetry 1^+ states in the even-even Xe isotopes as a function of the mass number A (see text). Upper part: Decay branching $R_{\text{exp},1}$ for the decay to the first excited 2^+ state. Lower part: Decay branching $R_{\text{exp},2}$ for the decay to the second excited 2^+ state. The full and dotted lines give the values as predicted by IBM-2 in the O(6) limit. The error bars of the data are smaller than the symbol sizes.

isotopic chains as a basic property of $M1$ excitations to 1^+ MS states. This dependence can be explained in several theoretical approaches (see, e.g., Ref. [82]). In Fig. 11 the $B(M1) \uparrow$ values for the seven even-even Xe isotopes are plotted against the corresponding β_2^2 data taken from the compilation of Raman *et al.* [83]. For the lighter isotopes $^{126,124}\text{Xe}$, which approach the O(6) limit, the $M1$ strengths seem to be somewhat fragmented, as expected. Therefore, the strengths were summed in narrow energy intervals, as indicated by the dashed lines in Fig. 4.

A first-order X(5) phase transition was observed experimentally in the $N = 90$ isotones [5,6,8]. The sudden jump of increased $B(E2)$ values causes, as already discussed, the deformation splitting of the higher lying electric GDR [10,11]. Because of the proportionality of $B(E2)$ and $B(M1)$ values [72] this also should influence the $M1$ strength distributions. However, the E(5) phase transition is expected to be of second order. The $B(E2)$ values in the Xe and Ba isotopes vary only smoothly and increase nearly linearly with decreasing neutron numbers (see, e.g., Ref. [58]). Therefore, it is not astonishing that no drastic changes were observed in the present dipole strength distributions in the Xe isotopes. Nevertheless, regarding the strengths of the $M1$ excitations to the 1^+ MS states (see Fig. 9), a change in the slope can be stated near $A = 128$ –130.

This behavior can be seen more clearly in Fig. 12. Here, in the upper part the experimental data for the $B(M1) \uparrow$ strengths are plotted as a function of the mass number A and fitted by an empirical step function:

$$B(M1) \uparrow = a + \frac{b}{1 + \exp \frac{c-A}{d}}. \quad (9)$$

The lower part shows the negative first derivative of this function, which exhibits a distinct maximum at $A = 130$. In contrast, the dotted lines representing the IBM-2 prediction [in the O(6) limit] show a smooth trend without any extrema. These findings may be interpreted as a hint at a possible influence of the E(5) phase transition, since also the E_4/E_2 energy ratios for $^{128,130}\text{Xe}$ lie near to the E(5) expectation value of 2.2 (see Fig. 1). It should be mentioned that Bonatsos *et al.* [84] recently derived a γ -rigid solution of the Bohr Hamiltonian ($\gamma = 30^\circ$), which explains spectroscopic quantities in close agreement to the E(5) predictions. Also in this picture, the experimental data are best described in the Xe region near $A = 130$.

However, it should be emphasized that obtaining a clear manifestation of the E(5) phase transition requires more spectroscopic information on the complete low-lying level scheme, including transition probabilities and the various branching ratios, as is already available for the best E(5) candidate, the neighboring isotope ^{134}Ba [9].

C. $E2$ excitations in the even-even isotopes $^{124-136}\text{Xe}$

The overwhelming majority of the excitations observed in the even-even Xe isotopes were of dipole character. In addition, several quadrupole excitations were also identified. The results for these $E2$ transitions are summarized in Table IX. In the

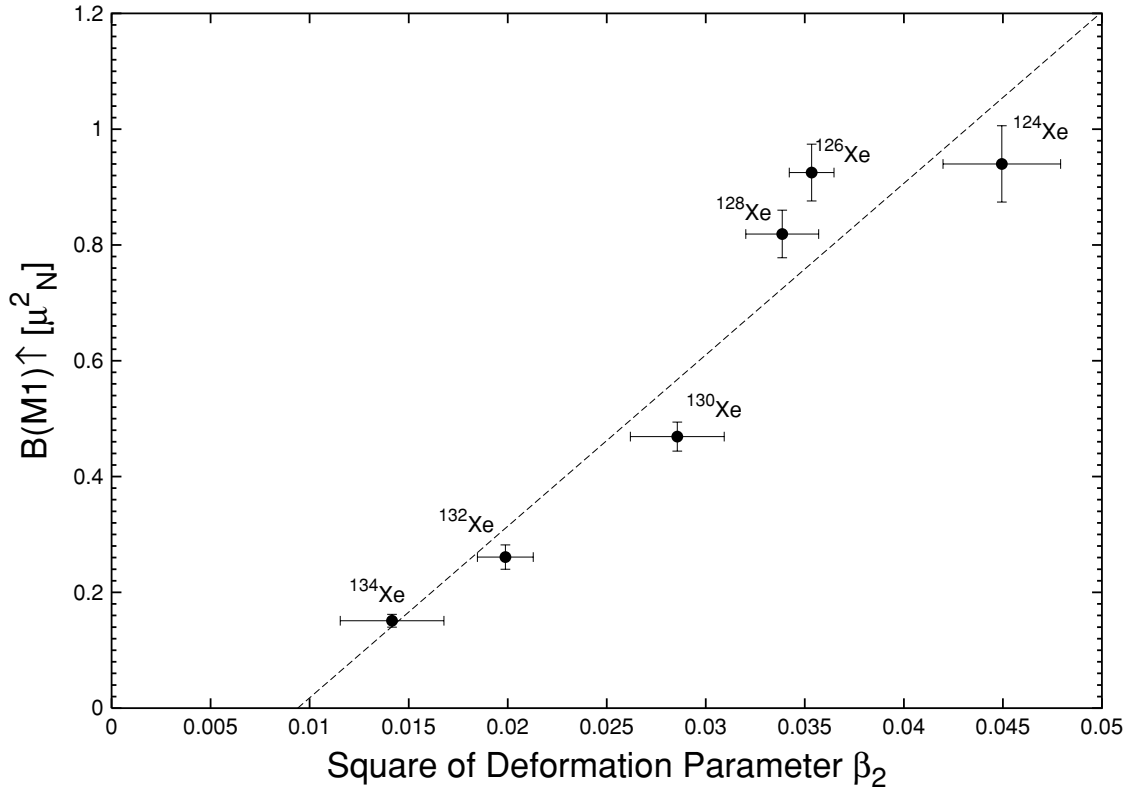


FIG. 11. Summed $B(M1) \uparrow$ strengths observed in the even-even Xe isotopes as a function of the squared deformation parameter β_2 . The dashed line represents a fit of a linear function to the data and serves to guide the eyes.

lightest isotope ^{124}Xe and in ^{128}Xe no $E2$ excitation was detected; in the neighboring isotope ^{126}Xe only one rather weak transition in the energy region of about 2.3 MeV could

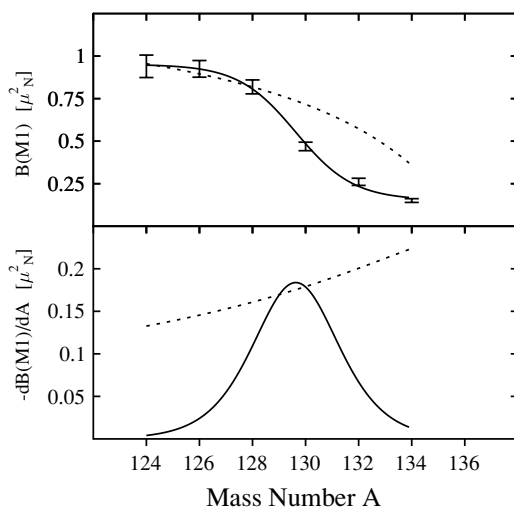


FIG. 12. Upper part: Summed $B(M1) \uparrow$ strengths observed in the even-even Xe isotopes as a function of the mass number A . The full line represents a fit of a step function to the data (see text). The dotted line shows the values predicted by the IBM-2 model in the $O(6)$ limit. Lower part: The first derivatives of both curves.

be observed. In contrast, for heavier isotopes, approaching the shell closure, several (up to six), $E2$ excitations could be identified. In the cases of ^{130}Xe and ^{136}Xe it was possible to detect a low-lying, rather strong transition at about 1100 and 1300 keV with excitation probabilities on the order of $1000 e^2 \text{fm}^4$, hinting at a collective character of these excitations. The excitations observed at higher energies are spread over the energy range of 1.8 to 3.7 MeV and are of reduced strengths on the order of 10 to $140 e^2 \text{fm}^4$. These results are reminiscent of and similar to the situation in the even-even Sn isotopes with their closed proton shell ($Z = 50$) [85].

In the energy range around 2 MeV the existence of the one-phonon 2^+ MS state is expected. This state was already identified in ^{128}Xe at an excitation energy of 2127 keV from its strong $M1$ transition to the 2^+_1 state [86]. In our experiment on ^{132}Xe we observed in the BGO-shielded 127° detector a γ -ray line at 1318 keV and a very weak line at 1985 keV that could stem from the decay of the known $J^\pi = 2^+_3$ state at 1985.6 keV [87] to the 2^+_1 and the ground state, respectively. However, the branching ratio for these decay transitions of $\Gamma_1/\Gamma_0 = 2.3(12)$ deviates from the value given in [87] of $\Gamma_1/\Gamma_0 = 10.0(21)$, where Γ_1 is the decay width of the decay transition to the 2^+_1 state. Using the branching ratio of the $2^+_3 \rightarrow 2^+_1$ transition of $\delta = -0.16(5)$ [87], we determine a large $M1$ transition strength of $B(M1, 2^+_3 \rightarrow 2^+_1) = 0.31(25)\mu_N^2$. The ground-state decay could represent a weakly collective $E2$

TABLE XIV. The summed $B(M1) \uparrow$ values experimentally observed in the odd-mass isotopes $^{129,131}\text{Xe}$ in comparison with those in the neighboring even-even Xe isotopes and theoretical expectations (see text).

Isotope	Energy (keV)	$\sum B(M1) \uparrow$ (exp.) (μ_N^2)	$B(M1) \uparrow$ (theor.) (μ_N^2)
128	2838	0.819(41)	0.819
129	2800±300	0.65(11)	—
	2800±500	1.17(15)	—
130	2763	0.469(25)	0.716
131	2739±300	0.246(78)	—
	2739±500	0.497(95)	—
132	2714	0.261(21)	0.573

transition with a transition strength of $B(E2, 2_3^+ \rightarrow 0_1^+) = 3.7(29)\text{W.u.}$ (corresponding to $B(E2) \uparrow = 740(580)e^2\text{fm}^4$). Therefore, the 2_3^+ state in ^{132}Xe presumably is a candidate for a one-phonon 2^+ MS state.

D. Dipole strength distributions in the odd-mass isotopes $^{129,131}\text{Xe}$

As can be seen in Fig. 6, the dipole strength distributions in the odd-mass isotopes $^{129,131}\text{Xe}$ are strongly fragmented in comparison to those in the neighboring even-even isotopes. For a more quantitative discussion, the strengths in the odd-mass isotopes are summed in energy ranges of ± 300 and 500 keV, respectively, around the average of the energies of the predominant $M1$ excitations in the even-even neighbors. This seems to be reasonable since these $M1$ excitations are really dominating the dipole strength distributions in the even-even neighbors. The numerical data of these summations are summarized in Table XIV and compared with the results in

the even-even neighbor isotopes and the theoretical predictions of the IBM-2 in the $O(6)$ limit. It can be stated that the integrated strengths observed in the odd-mass isotopes fit quite well into the systematics of the strengths detected in the neighboring even-even isotopes and are nicely described by IBM-2. Therefore, one may conclude that all fragments of the $M1$ excitations to MS states in the even-even nuclei were refound in the odd-mass isotopes experimentally.

VI. CONCLUSIONS

Systematic photon scattering experiments were performed on all nine stable Xe isotopes, the even-even isotopes $^{124,126,128,130,132,134,136}\text{Xe}$ and the two odd-mass isotopes $^{129,131}\text{Xe}$. The strongest dipole excitations in the even-even isotopes were ascribed to $M1$ transitions to 1^+ mixed-symmetry states. Their strengths in the lighter isotopes exhausts the IBM-2 predictions [in the $O(6)$ limit] and vanish when approaching the shell closure in ^{136}Xe . The trend of the strengths as a function of the mass number A provides a hint for a phase transition near $A = 130$. Candidates for $E1$ two-phonon excitations were observed in the heavier isotopes. Their strengths decrease steeply when moving away from the shell closure. In the odd-mass isotopes the dipole strength is rather fragmented. In the even-even isotopes several $E2$ excitations of weakly collective strengths were observed.

ACKNOWLEDGMENTS

Valuable discussions with Prof. R. V. Jolos (JINR Dubna) are gratefully acknowledged. This work was partially supported by the Deutsche Forschungsgemeinschaft (DFG) under Contract Nos. Kn 154/31, Br799/11, and Jo391/3-1. N.P. thanks the Department of Energy for his support under Grant No. DE-FGO2-04ER41334.

-
- [1] R. F. Casten, *Nuclear Structure from a Simple Perspective* (Oxford University Press, New York, 1990).
- [2] F. Iachello, Phys. Rev. Lett. **85**, 3580 (2000).
- [3] F. Iachello, Phys. Rev. Lett. **87**, 052502 (2001).
- [4] F. Iachello, Phys. Rev. Lett. **91**, 132502 (2003).
- [5] R. F. Casten and N. V. Zamfir, Phys. Rev. Lett. **87**, 052503 (2001).
- [6] R. Krücken, B. Albanna, C. Bialik, R. F. Casten, J. R. Cooper, A. Dewald, N. V. Zamfir, C. J. Barton, C. W. Beausang, M. A. Caprio, A. A. Hecht, T. Klug, J. R. Novak, N. Pietralla, and P. von Brentano, Phys. Rev. Lett. **88**, 232501 (2002).
- [7] R. Bijker, R. F. Casten, N. V. Zamfir, and E. A. McCutchan, Phys. Rev. C **68**, 064304 (2003).
- [8] D. Tonev, A. Dewald, T. Klug, P. Petkov, J. Jolie, A. Fitzler, O. Möller, S. Heinze, P. von Brentano, and R. F. Casten, Phys. Rev. C **69**, 034334 (2004).
- [9] R. F. Casten and N. V. Zamfir, Phys. Rev. Lett. **85**, 3584 (2000).
- [10] P. Carlos, H. Beil, R. Bergère, A. Leprêtre, A. de Miniac, and A. Veyssièrre, Nucl. Phys. **A225**, 171 (1974).
- [11] P. Carlos, H. Beil, R. Bergère, A. Leprêtre, and A. Veyssièrre, Nucl. Phys. **A172**, 437 (1971).
- [12] H. H. Pitz, R. D. Heil, U. Kneissl, S. Lindenstruth, U. Seemann, R. Stock, C. Wesselborg, A. Zilges, P. von Brentano, S. D. Hoblit, and A. M. Nathan, Nucl. Phys. **A509**, 587 (1990).
- [13] J. Margraf, R. D. Heil, U. Kneissl, U. Maier, H. H. Pitz, H. Friedrichs, S. Lindenstruth, B. Schlitt, C. Wesselborg, P. von Brentano, R.-D. Herzberg, and A. Zilges, Phys. Rev. C **47**, 1474 (1993).
- [14] T. Eckert, O. Beck, J. Besserer, P. von Brentano, R. Fischer, R.-D. Herzberg, U. Kneissl, J. Margraf, H. Maser, A. Nord, N. Pietralla, H. H. Pitz, S. W. Yates, and A. Zilges, Phys. Rev. C **56**, 1256 (1997); **57**, 1007(E) (1998).
- [15] U. Kneissl, H. H. Pitz, and A. Zilges, Prog. Part. Nucl. Phys. **37**, 349 (1996).
- [16] R.-D. Herzberg, I. Bauske, P. von Brentano, Th. Eckert, R. Fischer, W. Geiger, U. Kneissl, J. Margraf, H. Maser, N. Pietralla, H. H. Pitz, and A. Zilges, Nucl. Phys. **A592**, 211 (1995).

- [17] H. Maser, N. Pietralla, P. von Brentano, R.-D. Herzberg, U. Kneissl, J. Margraf, H. H. Pitz, and A. Zilges, *Phys. Rev. C* **54**, R2129 (1996).
- [18] N. Pietralla, D. Belic, P. von Brentano, C. Fransen, R.-D. Herzberg, U. Kneissl, H. Maser, P. Matschinsky, A. Nord, T. Otsuka, H. H. Pitz, V. Werner, and I. Wiedenhöver, *Phys. Rev. C* **58**, 796 (1998).
- [19] M. Scheck, H. von Garrel, N. Tsoneva, D. Belic, P. von Brentano, C. Fransen, A. Gade, J. Jolie, U. Kneissl, C. Kohstall, A. Linnemann, A. Nord, N. Pietralla, H. H. Pitz, F. Stedile, C. Stoyanov, and V. Werner, *Phys. Rev. C* **70**, 044319 (2004).
- [20] R. F. Casten, P. von Brentano, K. Heyde, P. van Isacker, and J. Jolie, *Nucl. Phys.* **A439**, 289 (1985).
- [21] V. Werner, H. Meise, I. Wiedenhöver, A. Gade, and P. von Brentano, *Nucl. Phys.* **A692**, 451 (2001).
- [22] U. E. P. Berg and U. Kneissl, *Annu. Rev. Nucl. Part. Sci.* **37**, 33 (1987).
- [23] N. Pietralla, I. Bauske, O. Beck, P. von Brentano, W. Geiger, R.-D. Herzberg, U. Kneissl, J. Margraf, H. Maser, H. H. Pitz, and A. Zilges, *Phys. Rev. C* **51**, 1021 (1995).
- [24] R. Reifarh, M. Heil, F. Käppeler, F. Voss, K. Wisshak, F. Bečvář, M. Kritčka, R. Gallino, and Y. Nagai, *Phys. Rev. C* **66**, 064603 (2002).
- [25] A. Degener, C. Bläsing, R. D. Heil, A. Jung, U. Kneissl, H. H. Pitz, H. Schacht, S. Schennach, R. Stock, and C. Wesselborg, *Nucl. Phys.* **A513**, 29 (1990).
- [26] B. Schlitt, U. Maier, H. Friedrichs, S. Albers, I. Bauske, P. von Brentano, R. D. Heil, R.-D. Herzberg, U. Kneissl, J. Margraf, H. H. Pitz, C. Wesselborg, and A. Zilges, *Nucl. Instrum. Methods Phys. Res. A* **337**, 416 (1994).
- [27] N. Pietralla, C. Fransen, D. Belic, P. von Brentano, C. Frießner, U. Kneissl, A. Linnemann, A. Nord, H. H. Pitz, T. Otsuka, I. Schneider, V. Werner, and I. Wiedenhöver, *Phys. Rev. Lett.* **83**, 1303 (1999).
- [28] W. Andrejtscheff, C. Kohstall, P. von Brentano, C. Fransen, U. Kneissl, N. Pietralla, and H. H. Pitz, *Phys. Lett.* **B506**, 239 (2001).
- [29] N. V. Zamfir, P. D. Cottle, R. F. Casten, S. Deylitz, A. Gollwitzer, G. Graw, R. Hertenberg, B. Valnion, G. Cata-Danil, J. Zhang, and W. T. Chou, *Phys. Rev. C* **55**, R1007 (1997).
- [30] J. Katakura and K. Kitao, *Nucl. Data Sheets* **97**, 765 (2002).
- [31] B. Singh, *Nucl. Data Sheets* **93**, 33 (2001).
- [32] Yu. V. Sergeev, *Nucl. Data Sheets* **71**, 557 (1994).
- [33] A. A. Sonzogni, *Nucl. Data Sheets* **95**, 837 (2002).
- [34] P. F. Mantica Jr., B. E. Zimmerman, W. B. Walters, J. Rikovska, and N. J. Stone, *Phys. Rev. C* **45**, 1586 (1992).
- [35] A. Gade, I. Wiedenhöver, J. Gableske, A. Gelberg, H. Meise, N. Pietralla, and P. von Brentano, *Nucl. Phys.* **A665**, 268 (2000).
- [36] E. W. Schneider, M. D. Glascock, W. B. Walters, and R. A. Meyer, *Phys. Rev. C* **19**, 1025 (1979).
- [37] R. G. Helmer, C. W. Reich, R. J. Gehrke, R. C. Greenwood, and R. A. Anderl, *Phys. Rev. C* **15**, 1453 (1977).
- [38] L. V. Groshev, L. I. Govor, A. M. Denisov, A. S. Rakhimov, *Sov. J. Nucl. Phys.* **13**, 647 (1971).
- [39] W. Gelletly, W. R. Krane, and D. R. MacKenzie, *Phys. Rev. C* **3**, 1678 (1971).
- [40] J. Ott, C. Doll, T. von Egidy, R. Georgii, W. Schauer, and H.-F. Wirth, *Fizika (Zagreb)* **B5**, 199 (1996).
- [41] W. G. Winn and D. G. Sarantites, *Phys. Rev.* **184**, 1188 (1969).
- [42] E. Achterberg, E. Y. de Aisenberg, F. C. Iglesias, A. E. Jech, J. A. Moragues, D. Otero, M. L. Pérez, A. N. Proto, J. J. Rossi, W. Scheuer, and J. F. Suárez, *Phys. Rev. C* **4**, 188 (1971).
- [43] W. R. Western, J. C. Hill, W. L. Talbert Jr., and W. C. Schick Jr., *Phys. Rev. C* **15**, 1822 (1977).
- [44] R. A. Gatenby, J. R. Vanhoy, E. M. Baum, E. L. Johnson, S. W. Yates, T. Belgia, B. Fazekas, Á. Veres, and G. Molnár, *Phys. Rev. C* **41**, R414 (1990).
- [45] J. R. Vanhoy, J. M. Anthony, B. M. Haas, B. H. Benedict, B. T. Meehan, S. F. Hicks, C. M. Davoren, and C. L. Lundstedt, *Phys. Rev. C* **52**, 2387 (1995).
- [46] A. Gade and P. von Brentano, *Phys. Rev. C* **66**, 014304 (2002).
- [47] P. E. Garrett, H. Lehmann, J. Jolie, C. A. McGrath, M. Yeh, and S. W. Yates, *Phys. Rev. C* **59**, 2455 (1999).
- [48] D. Bandyopadhyay, C. C. Reynolds, S. R. Lesner, C. Fransen, N. Boukharouba, M. T. McEllistrem, and S. W. Yates, *Phys. Rev. C* **68**, 014324 (2003).
- [49] A. Kumar, J. N. Orce, S. R. Leshner, C. J. McKay, M. T. McEllistrem, and S. W. Yates, *Phys. Rev. C* **72**, 034313 (2005).
- [50] P. Vogel and L. Kocbach, *Nucl. Phys.* **A176**, 33 (1971).
- [51] M. Wilhelm, E. Rademacher, A. Zilges, and P. von Brentano, *Phys. Rev. C* **54**, R449 (1996).
- [52] M. Wilhelm, S. Kasemann, G. Pascovici, E. Rademacher, P. von Brentano, and A. Zilges, *Phys. Rev. C* **57**, 577 (1998).
- [53] J. Bryssinck, L. Govor, D. Belic, F. Bauwens, O. Beck, P. von Brentano, D. De Frenne, T. Eckert, C. Fransen, K. Govaert, R.-D. Herzberg, E. Jacobs, U. Kneissl, H. Maser, A. Nord, N. Pietralla, H. H. Pitz, V. Y. Ponomarev, and V. Werner, *Phys. Rev. C* **59**, 1930 (1999).
- [54] I. Pysmenetska, S. Walter, J. Enders, H. von Garrel, O. Karg, U. Kneissl, C. Kohstall, P. von Neumann-Cosel, H. H. Pitz, V. Y. Ponomarev, M. Scheck, F. Stedile, and S. Volz, *Phys. Rev. C* **73**, 017302 (2006).
- [55] C. Kohstall, D. Belic, P. von Brentano, C. Fransen, A. Gade, R.-D. Herzberg, J. Jolie, U. Kneissl, A. Linnemann, A. Nord, N. Pietralla, H. H. Pitz, M. Scheck, F. Stedile, V. Werner, and S. W. Yates, *Phys. Rev. C* **72**, 034302 (2005).
- [56] R. Georgi, P. von Neumann-Cosel, T. von Egidy, M. Grinberg, V. A. Khitrov, J. Ott, P. Prokofjevs, A. Richter, W. Schauer, C. Schlegel, R. Schulz, L. J. Simonova, C. Stoyanov, A. M. Sukhovoij, and A. V. Vojnov, *Phys. Lett.* **B351**, 82 (1995).
- [57] R. Schwengner, G. Winter, W. Schauer, M. Grinberg, F. Becker, P. von Brentano, J. Eberth, J. Enders, T. von Egidy, R.-D. Herzberg, N. Huxel, L. Käubler, P. von Neumann-Cosel, N. Nicolay, J. Ott, N. Pietralla, H. Prade, S. Raman, J. Reif, A. Richter, C. Schlegel, H. Schnare, T. Sevene, S. Skoda, T. Steinhardt, C. Stoyanov, H. G. Thomas, I. Wiedenhöver, and A. Zilges, *Nucl. Phys.* **A620**, 277 (1997).
- [58] M. Scheck, H. von Garrel, N. Tsoneva, D. Belic, P. von Brentano, C. Fransen, A. Gade, J. Jolie, U. Kneissl, C. Kohstall, A. Linnemann, A. Nord, N. Pietralla, H. H. Pitz, F. Stedile, C. Stoyanov, and V. Werner, *Phys. Rev. C* **70**, 044319 (2004).
- [59] M. Grinberg and C. Stoyanov, *Nucl. Phys.* **A573**, 231 (1994).
- [60] V. Y. Ponomarev, C. Stoyanov, N. Tsoneva, and M. Grinberg, *Nucl. Phys.* **A635**, 470 (1998).
- [61] R. V. Jolos and W. Scheid, *Phys. Rev. C* **66**, 044303 (2002).
- [62] R. V. Jolos, N. Y. Shirikova, and V. V. Voronov, *Phys. Rev. C* **70**, 054303 (2004).
- [63] R. V. Jolos, N. Y. Shirikova, and V. V. Voronov, to be published and private communication (2005).

- [64] A. Arima, T. Otsuka, F. Iachello, and I. Talmi, *Phys. Lett.* **66B**, 205 (1977).
- [65] T. Otsuka, A. Arima, and F. Iachello, *Nucl. Phys.* **A309**, 1 (1978).
- [66] F. Iachello, *Phys. Rev. Lett.* **53**, 1427 (1984).
- [67] P. van Isacker, K. Heyde, J. Jolie, and A. Sevrin, *Ann. Phys. (NY)* **171**, 253 (1986).
- [68] N. Pietralla, T. Mizusaki, P. von Brentano, R. V. Jolos, T. Otsuka, and V. Werner, *Phys. Rev. C* **57**, 150 (1997).
- [69] N. Lo Iudice and F. Palumbo, *Phys. Rev. Lett.* **41**, 1532 (1978).
- [70] D. Bohle, A. Richter, W. Steffen, A. E. L. Dieperink, N. Lo Iudice, F. Palumbo, and O. Scholten, *Phys. Lett.* **137B**, 27 (1984).
- [71] A. Richter, *Prog. Part. Nucl. Phys.* **34**, 261 (1995).
- [72] N. Pietralla, P. von Brentano, R.-D. Herzberg, U. Kneissl, J. Margraf, H. Maser, H. H. Pitz, and A. Zilges, *Phys. Rev. C* **52**, R2317 (1995).
- [73] N. Pietralla, P. von Brentano, R.-D. Herzberg, U. Kneissl, N. Lo Iudice, H. Maser, H. H. Pitz, and A. Zilges, *Phys. Rev. C* **58**, 184 (1998).
- [74] J. Enders, P. von Neumann-Cosel, C. Rangacharyulu, and A. Richter, *Phys. Rev. C* **71**, 014306 (2005).
- [75] C. Fransen, N. Pietralla, Z. Ammar, D. Bandyopadhyay, N. Boukharouba, P. von Brentano, A. Dewald, J. Gableske, A. Gade, J. Jolie, U. Kneissl, S. R. Leshner, A. F. Lisetskiy, M. T. McEllistrem, M. Merrick, H. H. Pitz, N. Warr, V. Werner, and S. W. Yates, *Phys. Rev. C* **67**, 024307 (2003).
- [76] V. Werner, D. Belic, P. von Brentano, C. Fransen, A. Gade, H. von Garrel, J. Jolie, U. Kneissl, C. Kohstall, A. Linnemann, A. F. Lisetskiy, N. Pietralla, H. H. Pitz, M. Scheck, K.-H. Speidel, F. Stedile, and S. W. Yates, *Phys. Lett.* **B550**, 140 (2002).
- [77] C. Fransen, N. Pietralla, A. P. Tonchev, M. W. Ahmed, J. Chen, G. Feldman, U. Kneissl, J. Li, V. Litvinenko, B. Perdue, I. V. Pinayev, H. H. Pitz, R. Prior, K. Sabourov, M. Spraker, W. Tornow, H. R. Weller, V. Werner, Y. K. Wu, and S. W. Yates, *Phys. Rev. C* **70**, 044317 (2004).
- [78] A. Linnemann, C. Fransen, M. Gorska, J. Jolie, U. Kneissl, P. Knoch, D. Mücher, H. H. Pitz, M. Scheck, C. Scholl, and P. von Brentano, *Phys. Rev. C* **72**, 064323 (2005).
- [79] T. C. Li, N. Pietralla, C. Fransen, H. von Garrel, U. Kneissl, C. Kohstall, A. Linnemann, H. H. Pitz, G. Rainovski, A. Richter, M. Scheck, F. Stedile, P. von Brentano, P. von Neumann-Cosel, and V. Werner, *Phys. Rev. C* **71**, 044318 (2005).
- [80] W. Ziegler, C. Rangacharyulu, A. Richter, and C. Spieler, *Phys. Rev. Lett.* **65**, 2515 (1990).
- [81] W. Ziegler, N. Huxel, P. von Neumann-Cosel, C. Rangacharyulu, A. Richter, C. Spieler, C. De Coster, and K. Heyde, *Nucl. Phys.* **A564**, 366 (1993).
- [82] N. Lo Iudice and A. Richter, *Phys. Lett.* **B304**, 193 (1993).
- [83] S. Raman, C. W. Nestor Jr., and P. Tikkanen, *At. Data Nucl. Data Tables* **78**, 1 (2001).
- [84] D. Bonatsos, D. Lenis, D. Petrellis, P. A. Terziev, and I. Yigitoglu, *Phys. Lett.* **B621**, 102 (2005).
- [85] J. Bryssinck, L. Govor, V. Y. Ponomarev, F. Bauwens, O. Beck, D. Belic, P. von Brentano, D. De Frenne, T. Eckert, C. Fransen, K. Govaert, R.-D. Herzberg, E. Jacobs, U. Kneissl, H. Maser, A. Nord, N. Pietralla, H. H. Pitz, and V. Werner, *Phys. Rev. C* **61**, 024309 (2000).
- [86] I. Wiedenhöver, A. Gelberg, T. Otsuka, N. Pietralla, J. Gableske, A. Dewald, and P. von Brentano, *Phys. Rev. C* **56**, R2354 (1997).
- [87] Y. Khazov, A. A. Rodionov, S. Sakharov, and B. Singh, *Nucl. Data Sheets* **104**, 497 (2005).